Shear Strength of Initially Unsaturated Soil

Laboratory results

Date 03 December 2020

Dr. Stefano Muraro
MSc. Ching-Yu Chao
Dr. Ir. Wout Broere

TU Delft

Faculteit Civiele Techniek en Geowetenschappen

Technische Universiteit Delft

Note

This document contains the results of the experimental investigation. The first part of the laboratory investigation was conducted on undisturbed samples retrieved from the borehole B002 at the Maasdijk near Oijen (Dp. 592 – 593), while the second part was carried out on undisturbed samples retrieved from the borehole B202 at the IJsseldijk near Westervoort (Dp. 250 + 80)

Some of the test choices and elaboration of the results have been discussed with Prof. Cristina Jommi.

Content

1. INTRODUCTION

The following pages summarise the results of laboratory tests on initially unsaturated soil samples, in order to study the effects of unsaturated conditions on the shear strength of Dutch dykes. The study was commissioned to TU Delft by Deltares and Directorate-General for Public Works and Water Management within the project "Shear Strength of Initially Unsaturated Soil" Project Overstijgende Verkenning Macrostabiliteit (POVM 11204453-002). Field testing, field monitoring and laboratory tests are combined to obtain a comprehensive overview of the role of unsaturated conditions on the response of the upper soil layers and the implications for the design and the assessment procedures for slope stability of dykes. Monitoring instrumentation including tensiometers and volumetric water content sensors was installed above the phreatic surface at the IJsseldijk near Westervoort (Dp. 250 + 80) and at the Maasdijk near Oijen (Dp. 592 - 593). In addition, piezometers were installed in the saturated zone of the IJsseldijk location. Furthermore, cone penetration tests (CPT) and field vane tests (FVT) were repeated during the monitoring period to evaluate the field shear strength of the subsoil during the wet and the dry seasons.

2. STUDY AREAS

2.1 Maasdijk near Oijen

The investigation was carried out on the crest at the Maasdijk near Oijen as displayed in Figure 1.

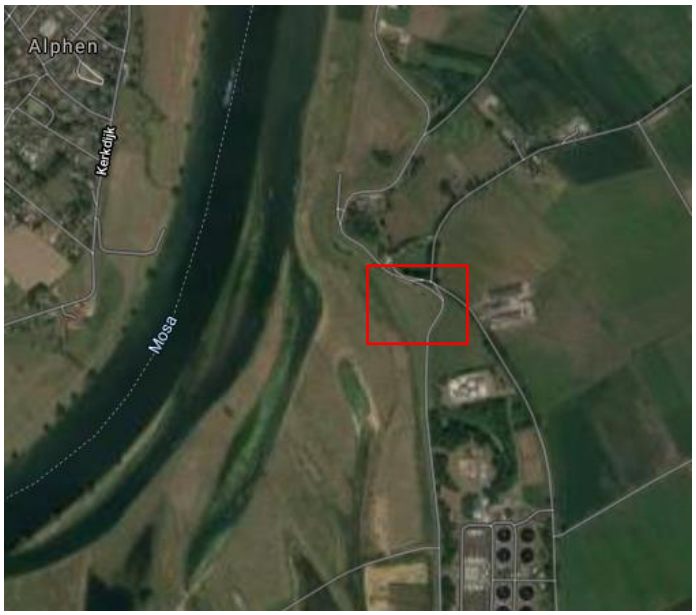

Figure 1. Test location at the Maasdijk near Oijen

The dyke, built in the 50s of the last century, is constructed using clay and sandy clay. The subsoil at the Maasdijk consists of 1.0 to 3.0 m thick Holocene clay layers and sandy clay layers on top of the Pleistocene sand layer (Grondmechanica Delft, 1996).

The field investigation carried out at the crest of dyke included:

- 2 boreholes: B001 retrieved on 25/09/2019 and B002 retrieved between 30/10/2019 and 01/11/2019; undisturbed samples were collected for soil classification and laboratory tests;
- CPT and FVT;
- 4 volumetric water content reflectometers CS616 of Campbell Scientific;
- 4 T5 tensiometers of Meter group.

The samples from the borehole B001 had been already used for soil classification by Ingenieurbureau Wiertsema & Partners bv. Samples from the borehole B002 have been used to perform the laboratory tests at TU Delft.

All the sensors were installed in separate boreholes drilled with a hand auger. The devices were installed with the probe rods in vertical direction. After installation, the boreholes were filled with bentonite. The installation depth of each sensor is reported in Table 1 and Table 2.

Table 1. Installation depth of the volumetric water content sensors at the Maasdijk near Oijen

Volumetric water content sensor	Depth NAP (m)	Depth from the ground (m)
W1	8.30	1.00
W2	7.58	1.70
W3	6.95	2.40
W4	6.19	3.10

Table 2. Installation depth of the tensiometers at the Maasdijk near Oijen

Tensiometer sensor	Depth NAP (m)	Depth from the ground (m)
T1	8.26	1.00
T2	7.63	1.70
T3	6.96	2.40
T4	6.19	3.10

The position of the sensors is displayed in Figure 2 together with the position of the sampling tubes from the borehole B002. The description from the field survey and after opening the tubes in the laboratory is also reported. The field survey located the phreatic surface at 5.3 m NAP with an excursion between 4.5 m and 5.8 m NAP as reported in Figure 2 for the sake of clarity.

Sensors position and borehole B002	Field description	Laboratory description
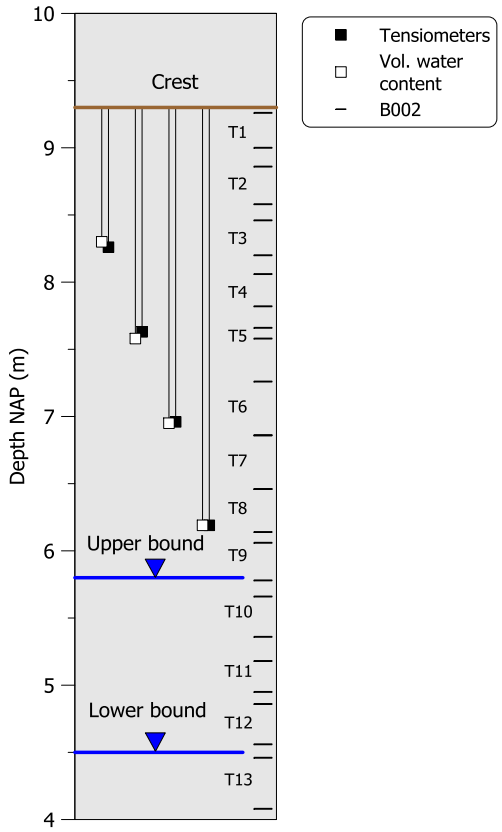	T2 to T5 Klei, matig siltig, zwak humeus, matig stevig T6 Klei, zwak zandig, zwak humeus, matig slap T7 Klei, matig siltig, matig slap T8 Klei, matig siltig, matig humeus, matig slap T9 Klei, matig siltig, sterk humeus, matig slap T13 Klei, matig siltig, matig humeus, matig stevig	T1 Silty clay T2 Silty clay T3 Silty clay T4 Silty clay T6 Sandy (undisturbed testing not possible except 1 sample) T7 top-mid sandy (undisturbed testing not possible), bottom silty clay T8 Silty clay T9 Sandy (undisturbed testing not possible) T13 Silty clay

Figure 2. Position of the sensors and the samples from the borehole B002 at the Maasdijk near Oijen with the description of the soil in the field and in the laboratory

2.2 IJsseldijk near Westervoort

The investigation was carried out on the inner berm at the IJsseldijk near Westervoort as displayed in Figure 3.

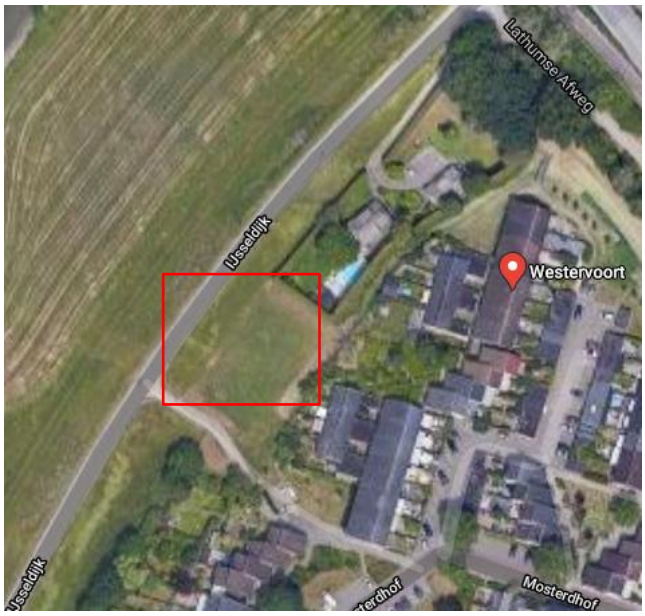

Figure 3. Test location at the IJsseldijk near Westervoort

The subsoil at the IJsseldijk consist of about 4.0 m thick Holocene clayey layers and sandy clay layers. These clayey layers lie on top of the Pleistocene sand layer (Inpijn-Blokpoel, 2017). The field investigation of relevance for the laboratory tests was carried out at the inner berm of the dyke and included:

- 2 boreholes: B201 retrieved on 31/10/2019 and B202 retrieved on 11/08/2020; undisturbed samples were collected for soil classification and laboratory tests;
- CPT and FVT;
- 4 volumetric water content reflectometers CS616 of Campbell Scientific;
- 4 T5 tensiometers of Meter group;
- 5 piezometers Geokon 4500DP.

The samples from the borehole B201 had been already used for soil classification by Ingenieurbureau Wiertsema & Partners bv. Samples from the borehole B202 have been used to perform the laboratory tests at TU Delft.

All the sensors were installed in separate boreholes drilled with a hand auger. The devices were installed with the probe rods in vertical direction. After installation, the boreholes were filled with bentonite. The installation depth of each sensor is reported in Table 3, Table 4, and Table 5.

Table 3. Installation depth of the volumetric water content sensors at the inner berm at the IJsseldijk near Westervoort

Volumetric water content sensor	Depth NAP (m)	Depth from the ground (m)
W9	9.40	1.00
W10	8.87	1.50
W11	8.41	2.00
W12	7.90	2.50

Table 4. Installation depth of the tensiometers at the inner berm at the IJsseldijk near Westervoort

Tensiometer sensor	Depth NAP (m)	Depth from the ground (m)
T9	9.35	1.00
T10	8.86	1.50
T11	8.37	2.00
T12	7.88	2.55

Table 5. Installation depth of the piezometers at the inner berm at the IJsseldijk near Westervoort

Piezometer	Depth NAP (m)	Depth from the ground (m)
P11	7.25	3.14
P12	6.74	3.65
P13	6.19	4.12
P14	5.69	4.64
P15	5.22	5.10

The position of the sensors is displayed in Figure 4 together with the position of the sampling tubes from the borehole B202. The description from the field survey and after opening the tubes in the laboratory is also reported. The field survey located the phreatic surface at 8.6 m NAP with an excursion between 8.3 m and 9.3 m NAP as reported in Figure 4 for the sake of clarity.

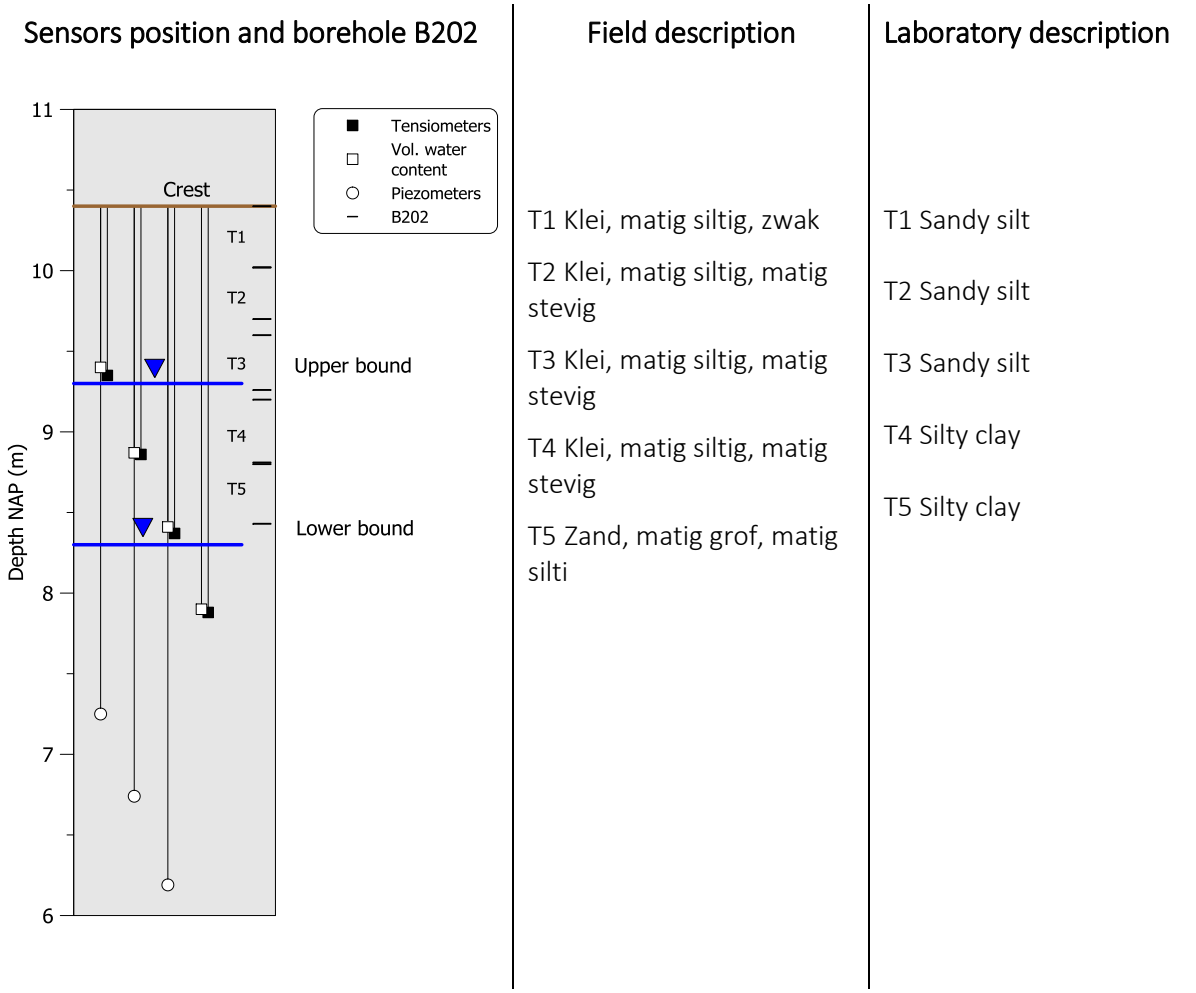

Figure 4. Position of the sensors and the samples from the borehole B202 in the inner berm at the IJsseldijk near Westervoort with the description of the soil in the field and in the laboratory

3. FIELD TESTS AND MONITORING

3.1. Cone penetration tests at the Maasdijk near Oijen

Multiple cone penetration tests were performed to quantify the variation of the in-situ shear strength during different periods both in the dry and wet season. Figure 5 displays the undrained shear strength, s_u, for a period ranging from 18/09/2019 to 11/05/2020. For each period, two tests are performed (series 1 and series 2 in Figure 5). The undrained shear strength is estimated from the CPT as

$$s_u = \frac{q_c - \sigma_v}{N_{kt}} \quad (1)$$

where q_c is the tip resistance, σ_v is the total vertical overburden stress and N_{kt} is set equal to 15 (van Duinen, 2020). A constant total unit weight of 18.7 kN/m^3 was assumed (van Duinen, 2020).

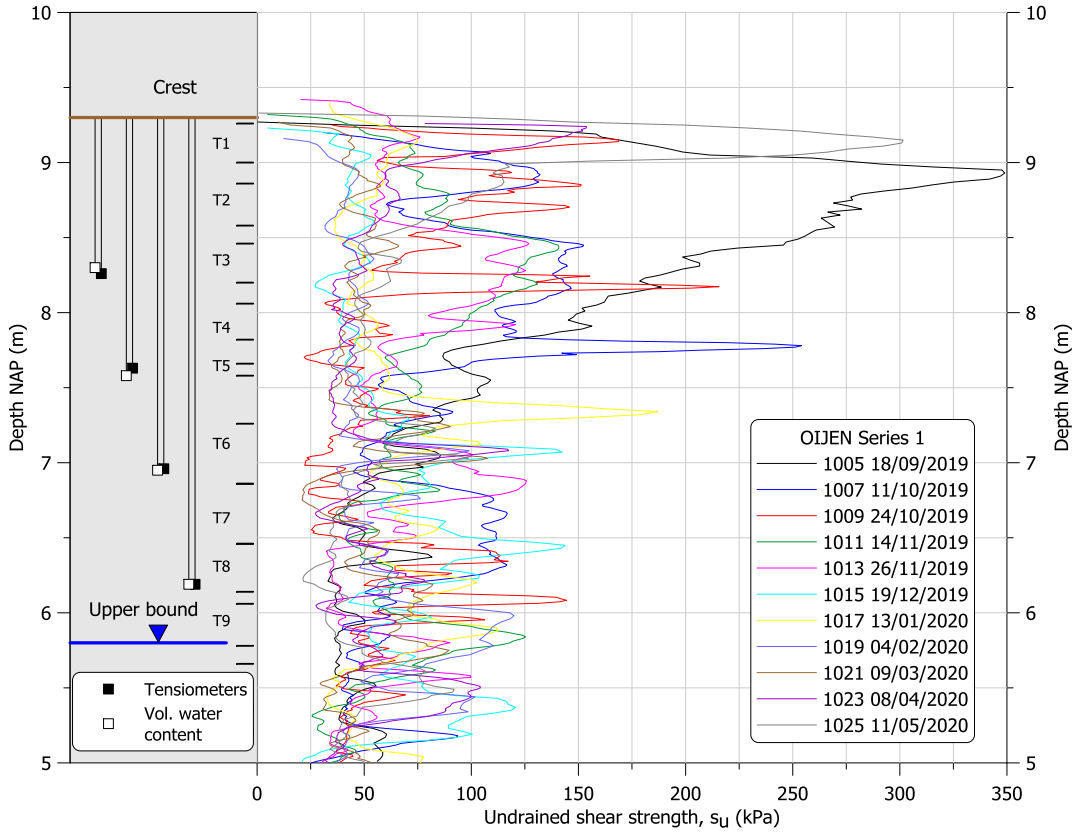

(a)

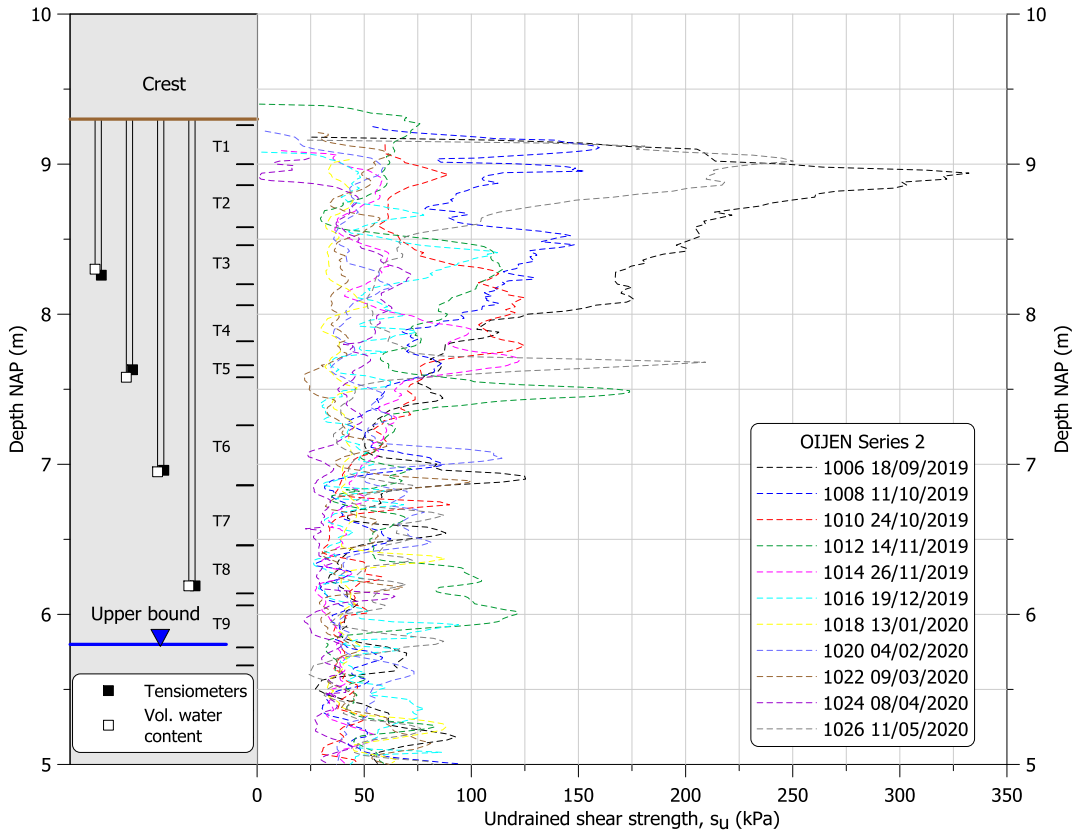

(b)

Figure 5. Profiles of the undrained shear strength estimated from CPT tests at the Maasdijk near Oijen

As shown in Figure 5, despite a quite strong inherent variability of the shear strength profile, the estimated undrained shear strength in the first two meters, from 9 to 7 m +NAP, presents remarkable variations during the monitoring period. For the sake of clarity, the daily precipitation records from the station at Megen (station code 903, 51.82N, 5.56E, KNMI) located 6 km east and the station at Volkel, 25 km south of Oijen (station code 375, 51.65N, 5.70E, KNMI) are displayed in Figure 6.

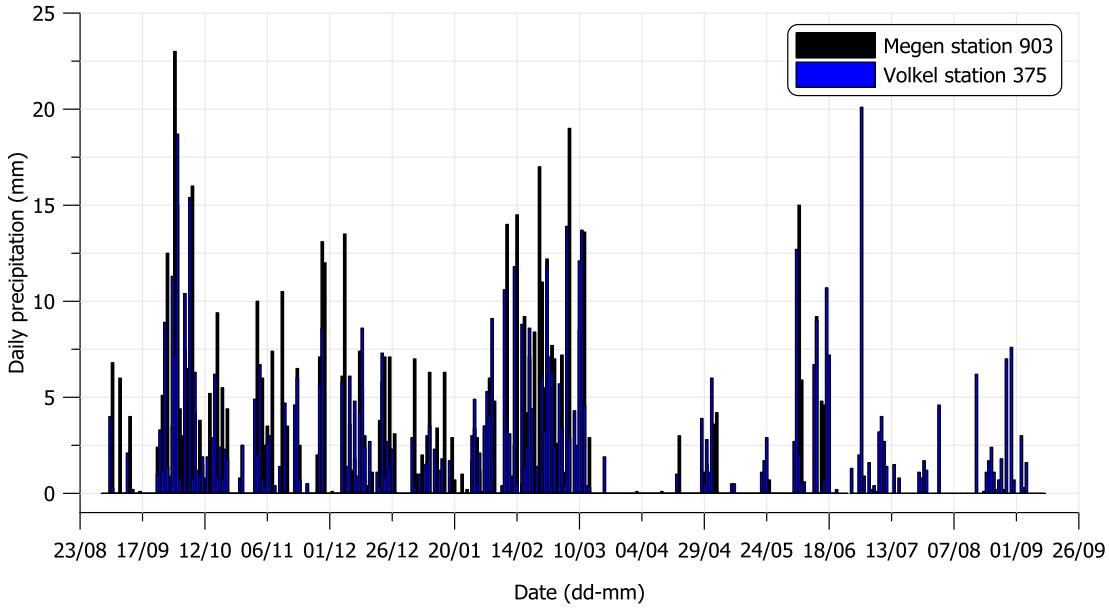

Figure 6. Daily precipitation recorded at the weather station at Megen and Volkel from 01/09/2019 to 12/09/2020 (Megen station available until 20/06/2020)

Two representative periods are selected namely: September 2019 to December 2019 and March 2020 to May 2020. As displayed in Figure 6, the first period corresponds to a transition from a very dry condition (September 2019) to a very wet condition (December 2019). On the contrary, the second period corresponds to a transition from a wet period (March 2020) to a dry period (May 2020). The corresponding profiles of the undrained shear strength in the field are displayed in Figure 7 (dry → wet) and Figure 8 (wet → dry). A dramatic reduction in the undrained shear strength occurred in the first 2 m of soil after the intense precipitation in October 2019 which dropped from values above 250 kPa to 40 kPa (Figure 7). On the contrary, the drying period experienced in spring 2020 contributed to increase the undrained shear strength from 50 kPa to values above 200 kPa (Figure 8).

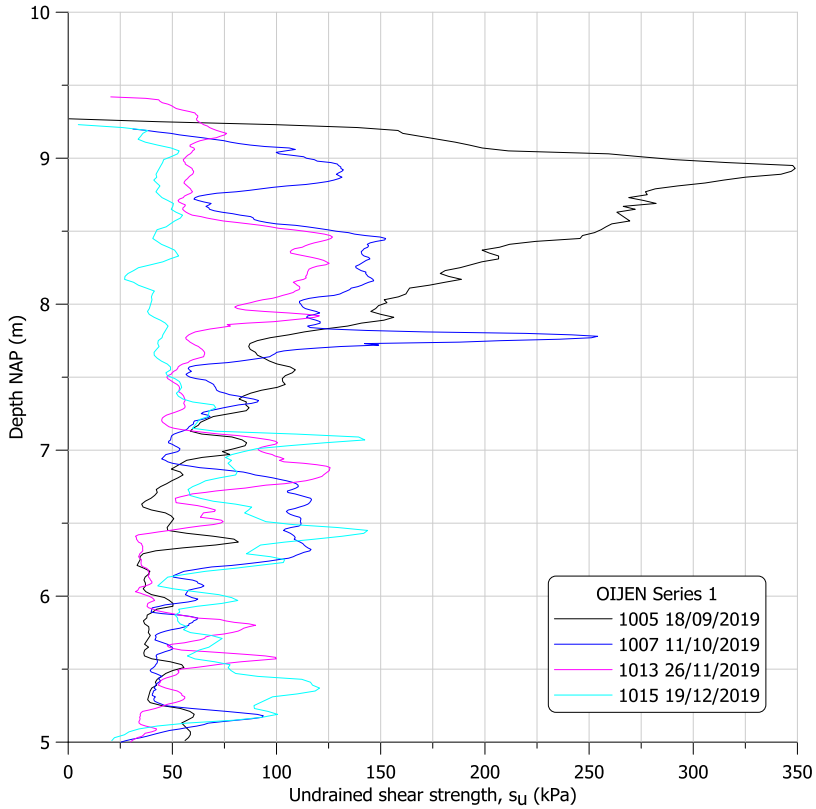

Figure 7. Profiles of the undrained shear strength at the Maasdijk near Oijen from 18/09/2019 to 19/12/2019 (dry → wet)

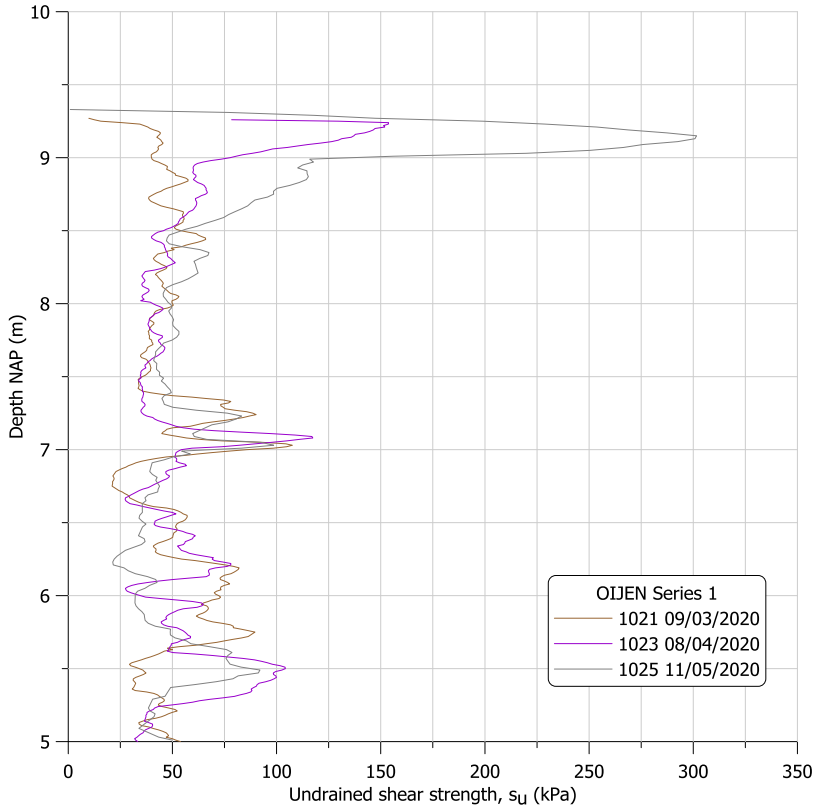

Figure 8. Profiles of the undrained shear strength at the Maasdijk near Oijen from 09/03/2020 to 11/05/2020 (wet → dry)

3.2. Water content measurements at the Maasdijk near Oijen

The evolution of the volumetric water content, θ, recorded at the Maasdijk near Oijen at different depths is displayed in Figure 9 together with the daily precipitation at Volkel station for the sake of clarity. The sensors were installed on 3rd October 2019.

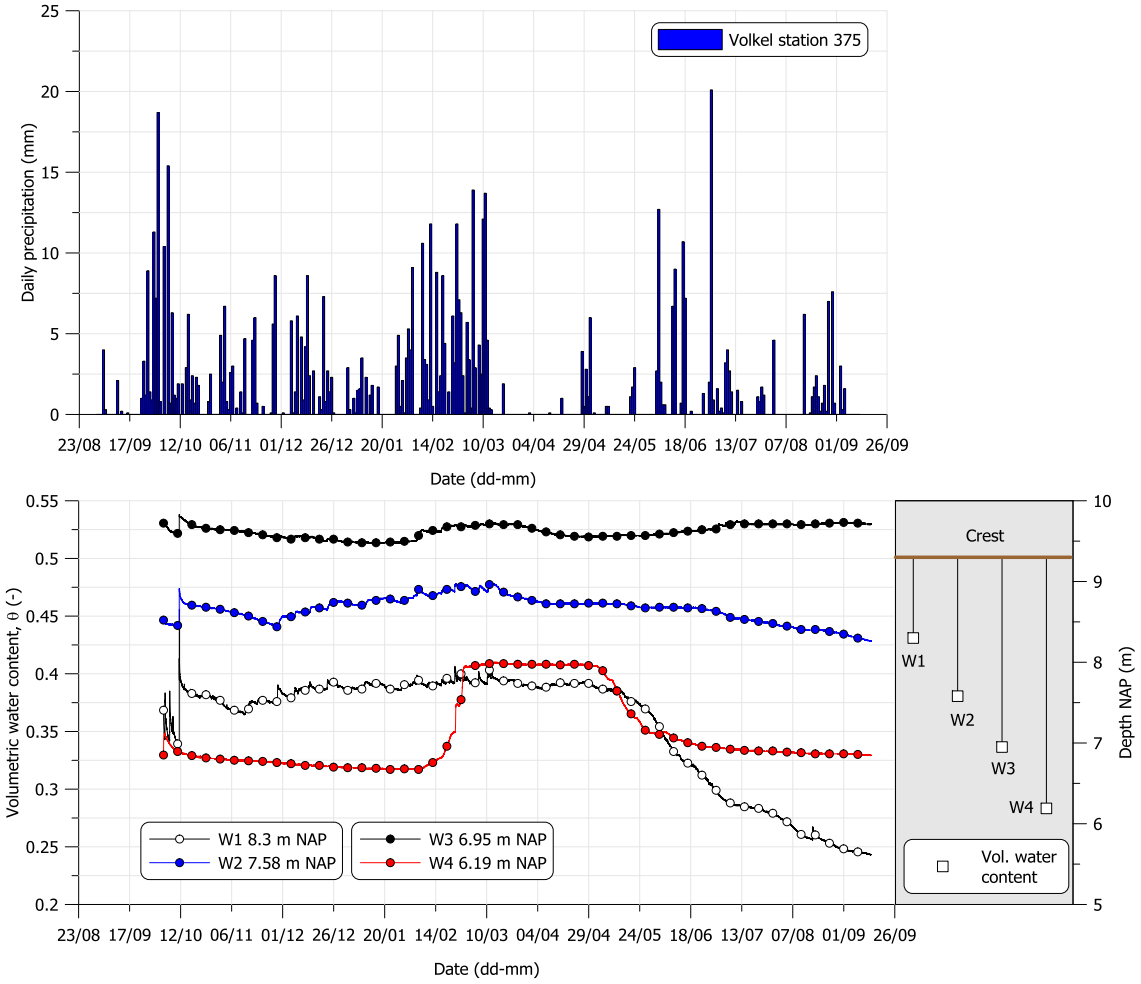

Figure 9. Volumetric water content measured at the Maasdijk near Oijen

As shown in Figure 9 the sensors were installed during the intense precipitation period in October 2019. The first two weeks the measurements showed some oscillations before the sensors reached equalisation. During the second intense precipitation period in February 2020, the sensors recorded a small increase in the volumetric water content followed by a decrease during the spring 2020, which is very clear in the shallowest sensor, W1, 1 m below the ground surface. The gravimetric water content, w, calculated with the dry density from the classification tests carried out in the borehole B001 by Wiertsema & Partners bv and assuming negligible volumetric strain is displayed in Figure 10.

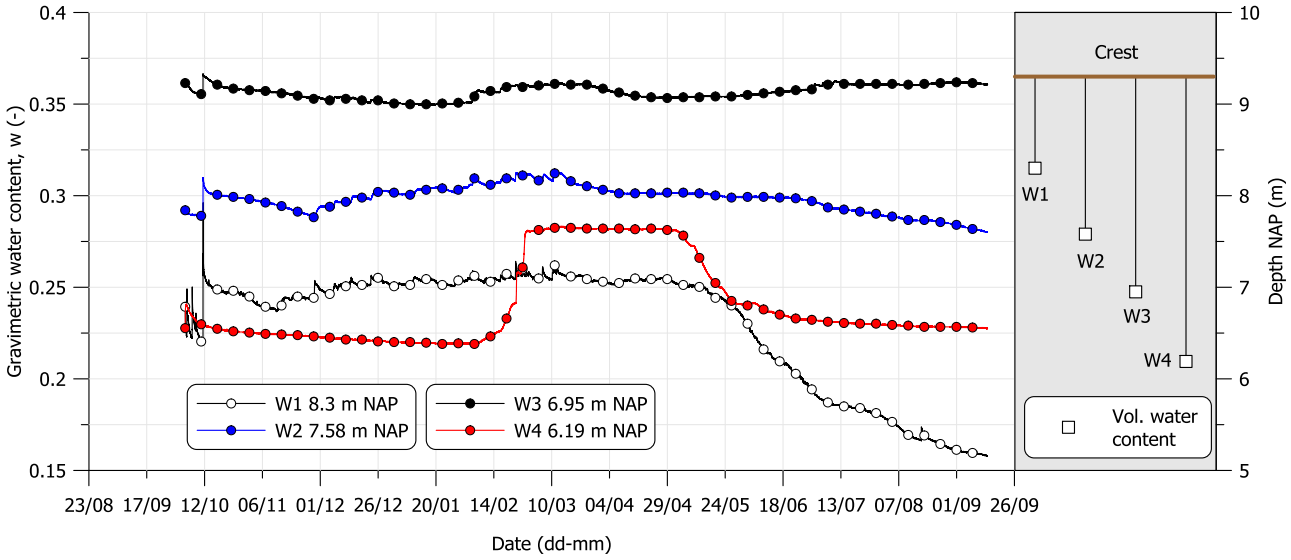

Figure 10. Gravimetric water content calculated from the field measurements and laboratory data at the Maasdijk near Oijen

3.3. Suction measurements at the Maasdijk near Oijen

The measurements of the pore water pressure from the tensiometers installed at the Maasdijk near Oijen are reported in Figure 11.

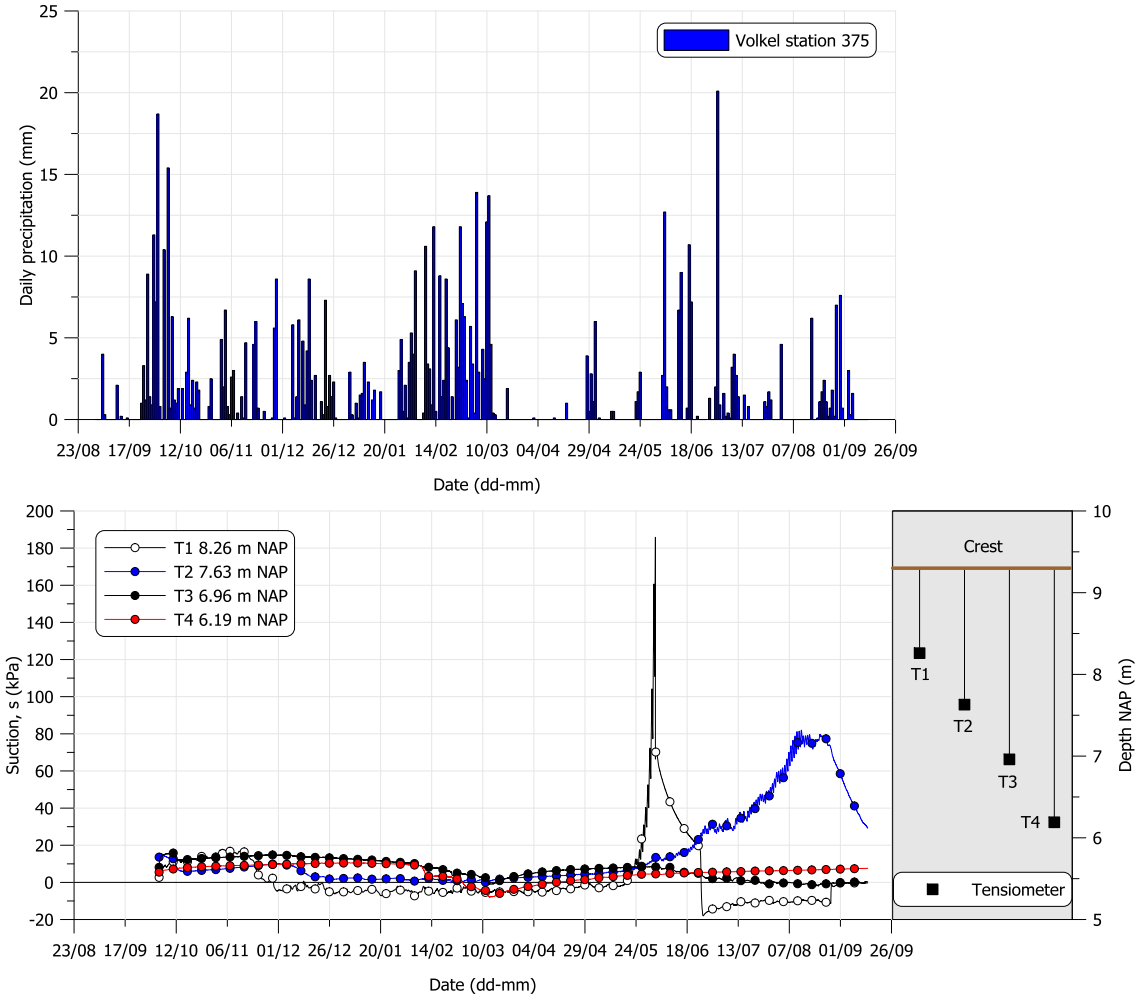

Figure 11. Suction measurements at the Maasdijk near Oijen

Similarly to the water content sensors, the tensiometers showed some fluctuation for the first two weeks after installation. With reference to the rainfall recorded at Volkel, the intense precipitation in late autumn and winter 2019 caused almost null suction in the upper part of the soil (T1 and T2). The tensiometers T1 and T2 showed a noticeable increase in suction starting from spring 2020. The most surficial tensiometer, 1 m below the ground, reached a maximum suction of about 180 kPa in early June while the sensor T2 at 7.6 m NAP cavitated at about 80 kPa later on in August. The deepest sensors T3 and T4 did not show significant suction development.

3.4. Cone penetration tests at the IJsseldijk near Westervoort

Multiple cone penetration tests were performed to quantify the variation of the in-situ shear strength during different periods both in the dry and wet seasons. Figure 12 displays the undrained shear strength, s_u, for a period ranging from 31/10/2019 to 11/05/2020. For each period, two tests are performed (series 1 and series 2 in Figure 12). The undrained shear strength is estimated from equation (1) with N_{kt} equal to 12.5 and a constant total unit weight of 18 kN/m^3 (van Duinen, 2020).

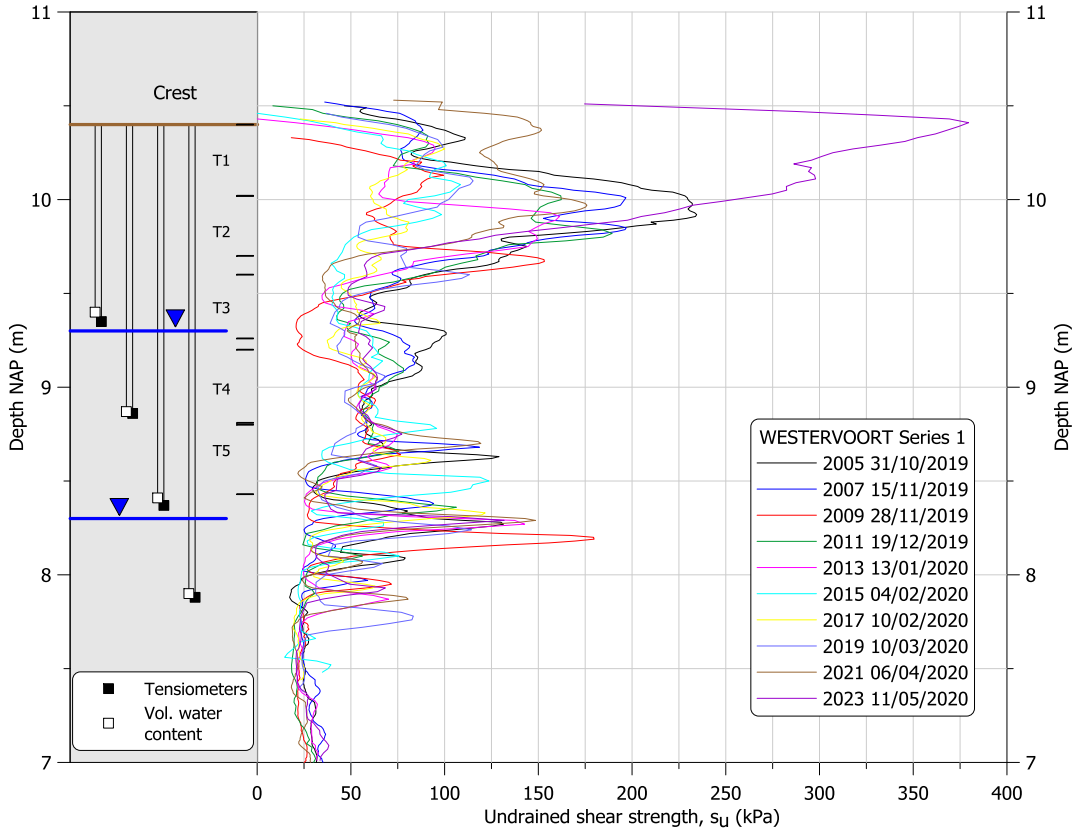

(a)

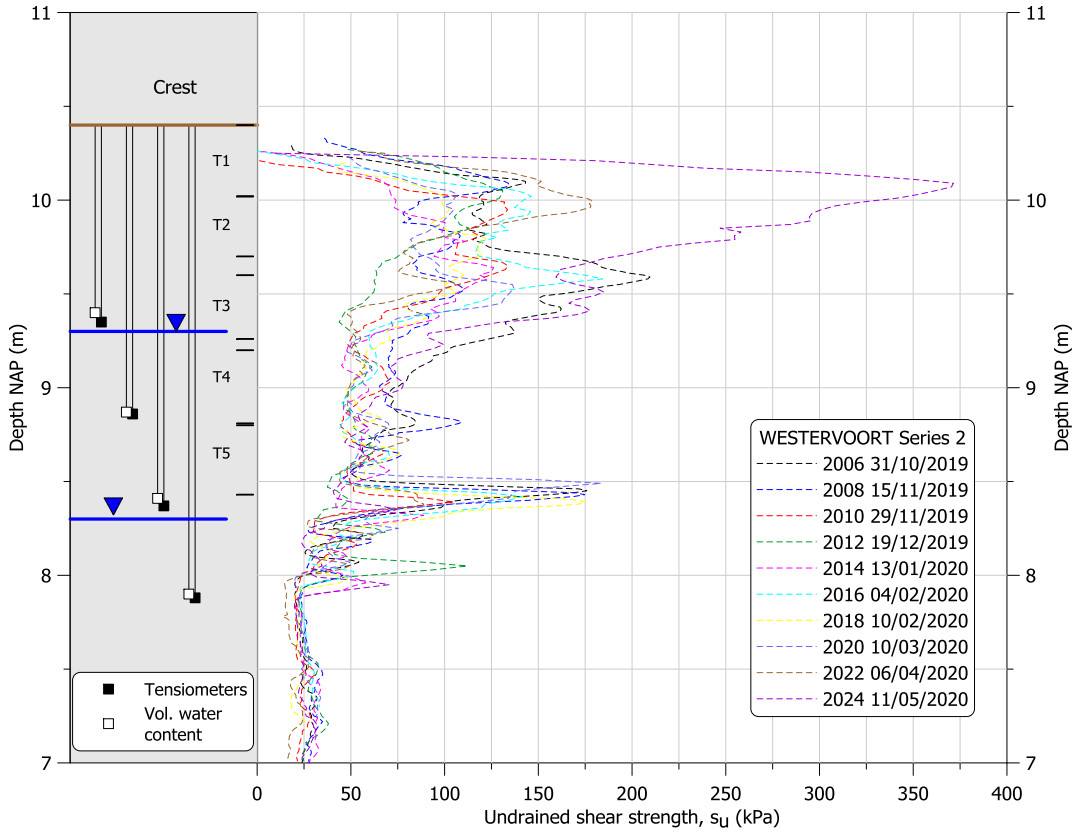

(b)

Figure 12. Profiles of the undrained shear strength estimated from CPT tests at the IJsseldijk near Westervoort

As shown in Figure 12, the estimated undrained shear strength in the first meter, from 10.4 to 9.4 m NAP, presents remarkable variations during the monitoring period. For the sake of clarity, the daily precipitation record from the station at Deelen (station code 275, 52.03N, 5.52E, KNMI) located 20 km north-west is displayed in Figure 13.

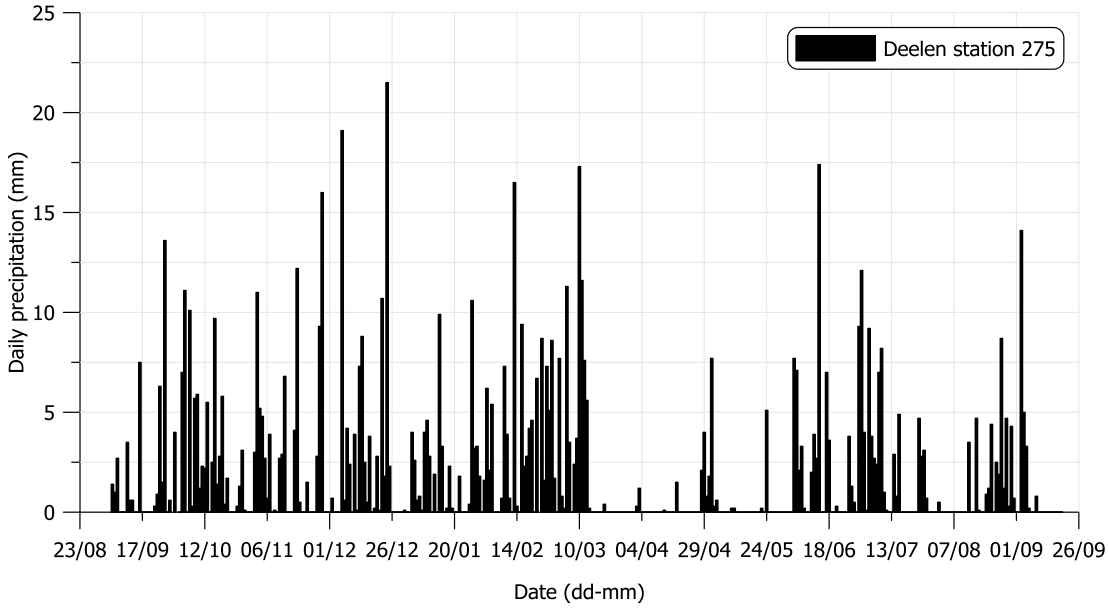

Figure 13. Daily precipitation recorded at the weather station at Deelen from 01/09/2019 to 19/09/2020

Two representative periods are selected namely: November 2019 to February 2020 and March 2020 to May 2020. The first period corresponds to a transition from a dry condition (November 2019) to a wet condition (February 2020). On the contrary, the second period corresponds to a transition from a wet period (March 2020) to a dry period (May 2020). The corresponding profiles of the undrained shear strength in the field are displayed in Figure 14 (dry → wet) and Figure 15 (wet → dry). A dramatic reduction in the undrained shear strength occurred in the first meter of soil after the intense precipitation in winter 2019 which dropped from values above 200 kPa to 50 kPa (Figure 14). On the contrary, the drying period experienced in spring 2020 contributed to increase the undrained shear strength from 70 kPa to values above 250 kPa (Figure 15).

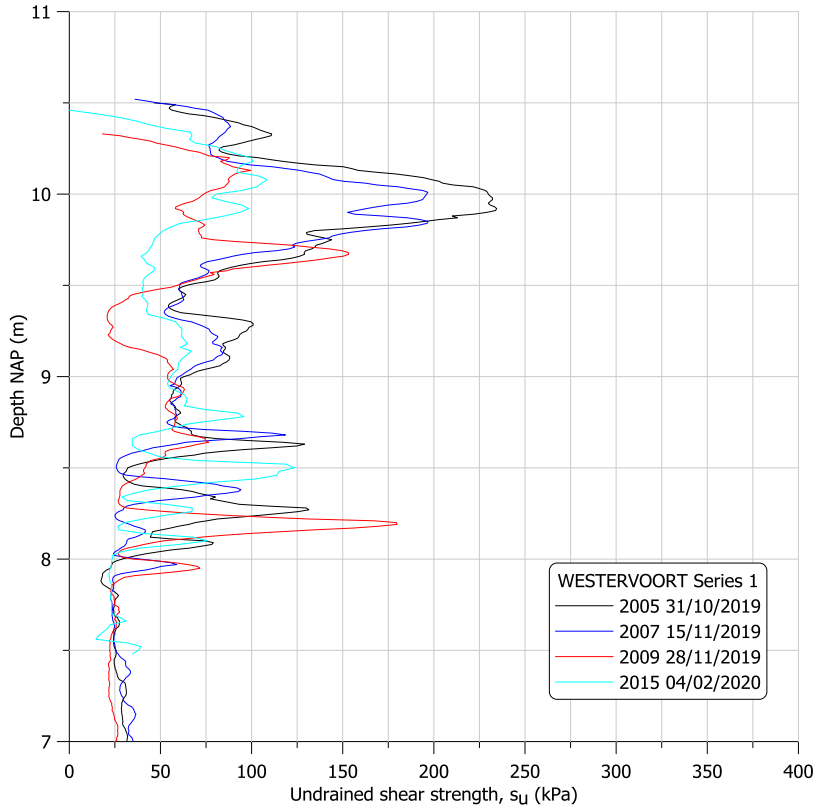

Figure 14. Profiles of the undrained shear strength at the IJsseldijk near Westervoort from 31/10/2019 to 04/02/2020 (dry → wet)

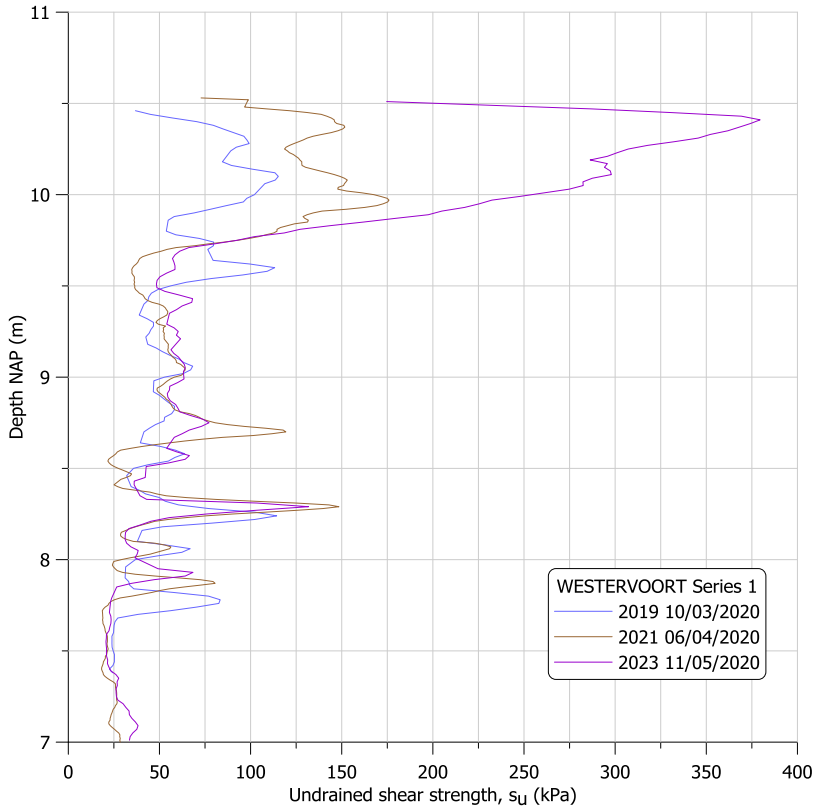

Figure 15. Profiles of the undrained shear strength at the IJsseldijk near Westervoort from 10/03/2020 to 11/05/2020 (wet → dry)

3.5. Water content measurements at the IJsseldijk near Westervoort

The evolution of the volumetric water content, θ, recorded at the inner berm at the IJsseldijk near Westervoort at different depths is displayed in Figure 16 together with the daily precipitation at Deelen station for the sake of clarity. The sensors were installed on 31st October 2019.

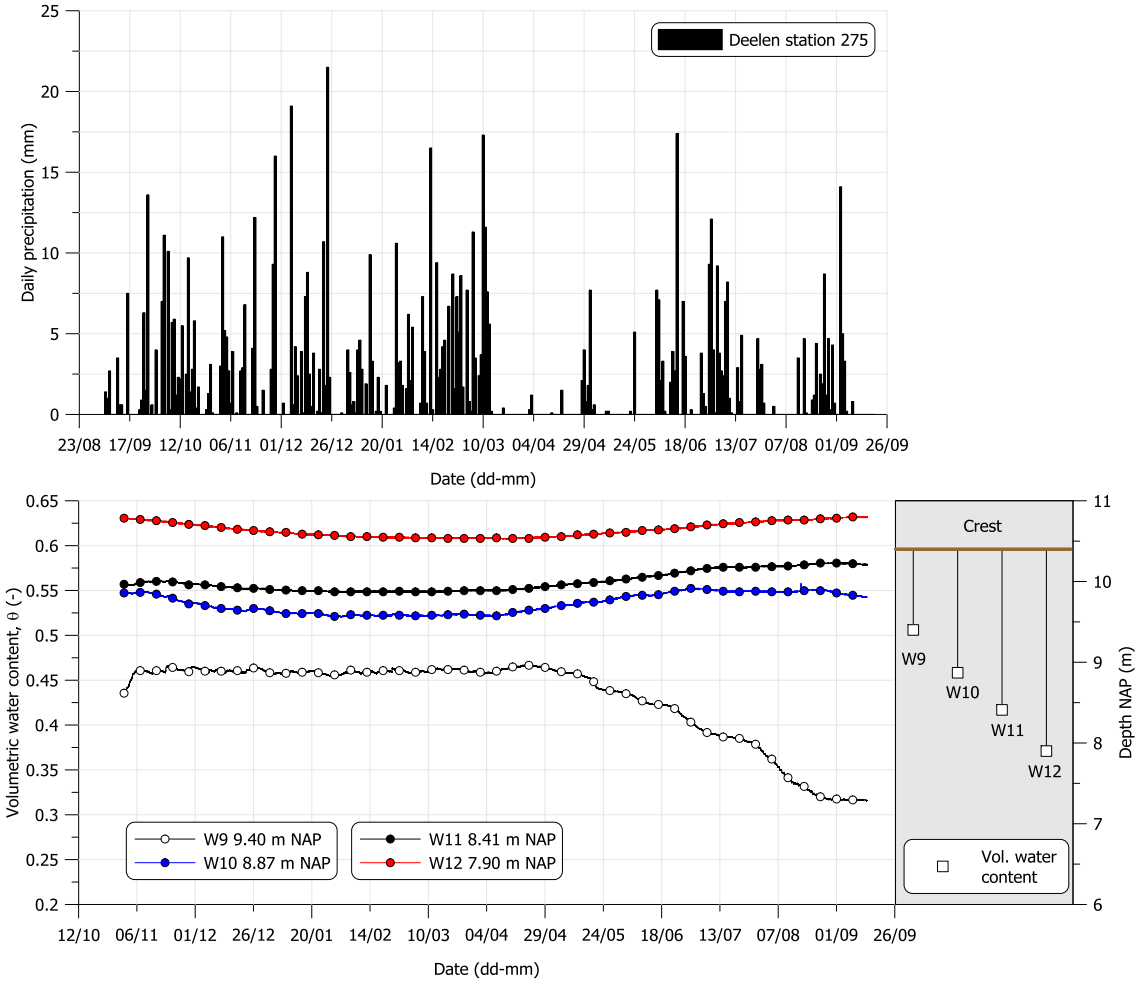

Figure 16. Volumetric water content measured at the inner berm at the IJsseldijk near Westervoort

The first two weeks the measurements showed some oscillations before the sensors reached equalisation. After March 2020, a very dry period occurred. Only the very shallow sensor, W9, 1 m below the ground surface, recorded a decrease in the volumetric water content. The gravimetric water content, w, calculated with the dry density from the classification tests carried out in the borehole B201 by Wiertsema & Partners bv and assuming negligible volumetric strain, is displayed in Figure 17.

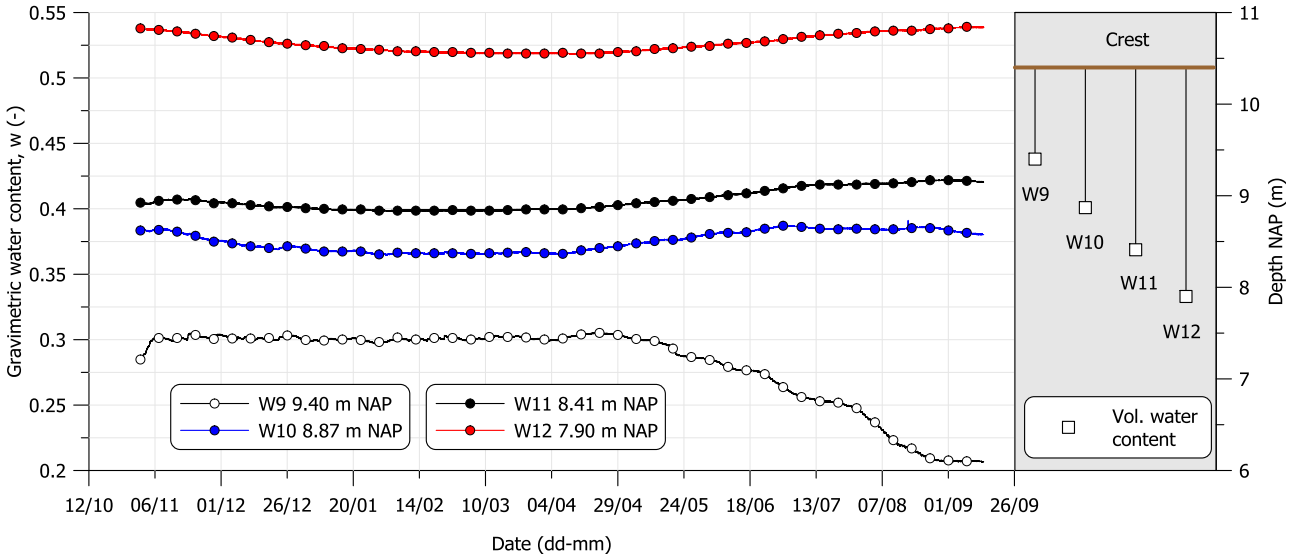

Figure 17. Gravimetric water content calculated from the field measurements and laboratory data at the inner berm at the IJsseldijk near Westervoort

3.6. Suction measurements at the IJsseldijk near Westervoort

The measurements of the pore water pressure from the tensiometers installed at the inner berm at the IJsseldijk near Westervoort are reported in Figure 18.

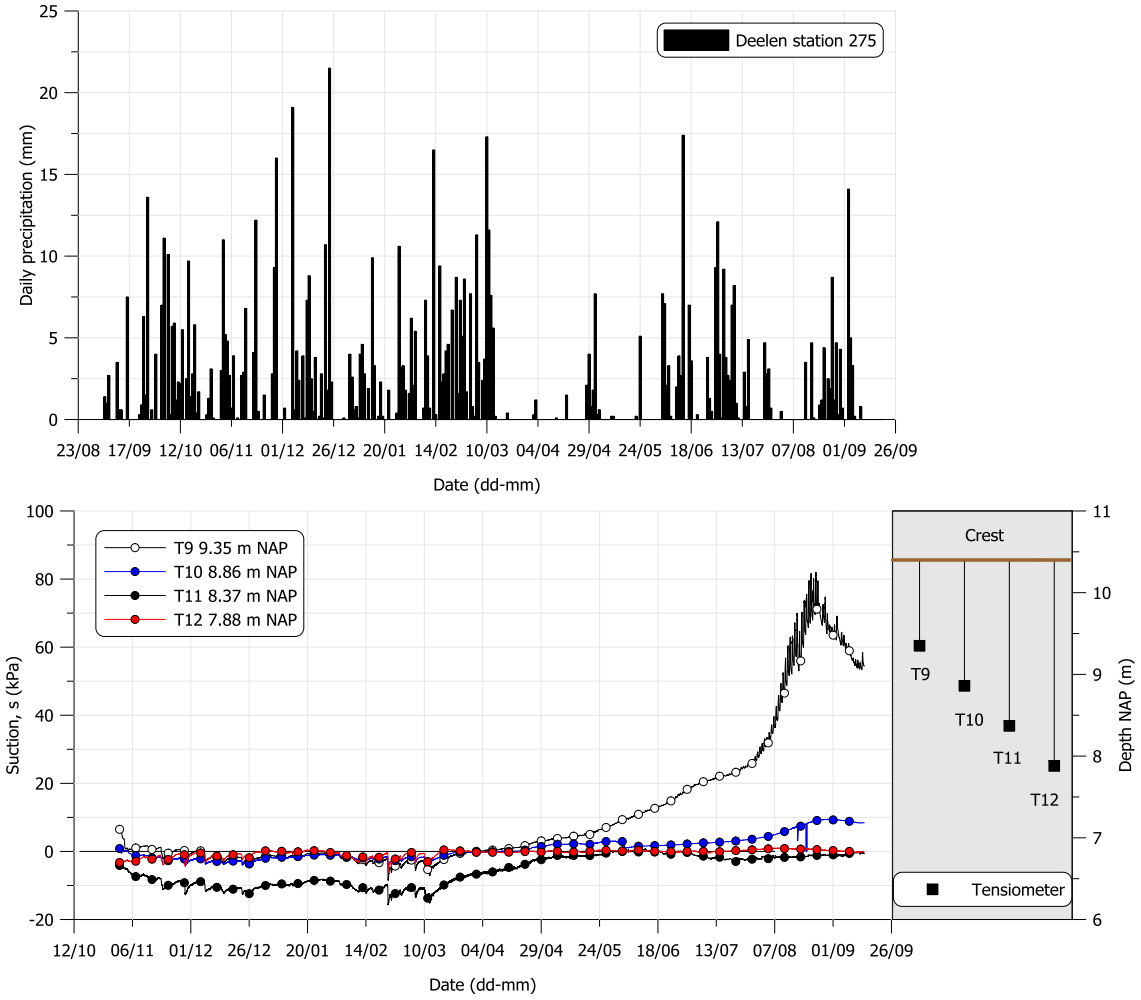

Figure 18. Suction measurements at the IJsseldijk near Westervoort

Similarly to the water content sensors, the tensiometers showed some fluctuation for the first two weeks after installation. With reference to the rainfall recorded at Deelen, the intense precipitation in late autumn and winter 2019 caused null suction in the upper part of the soil (T9 and T10). The tensiometer T9 showed a noticeable increase in suction starting from spring 2020 which reached a maximum of about 80 kPa in late August. The sensor T10 showed a small increase in suction in August 2020 while the deepest sensors T11 and T12 did not show significant suction development.

4. LABORATORY TESTS AT THE MAASDIJK NEAR OIJEN

4.1. Introduction

The laboratory tests are conducted on undisturbed samples from the borehole B002 retrieved in the very wet period between the 31/10/2019 and 01/11/2019. Samples from two depths are tested in two subsequent investigation stages. Over stage 1, the soil between 6.2 m and 7.3 m NAP is tested (Tube 6, 7, 8), while the stage 2 includes tests on the upper part of the dyke body between 7.8 m and 9.1 m NAP (Tube 1, 2, 3, 4). In the following the results collected during stage 1 and stage 2 are presented (Table 6 and Table 7 respectively).
The tests performed in stage 1 include:

- 2 unconsolidated undrained triaxial compression tests at natural water content (UU-n);
- 1 unconsolidated undrained triaxial compression test at dry condition (UU-d);
- 1 unconsolidated undrained triaxial compression test on a sample after drying and wetting cycle (UU-dw);
- 2 Hyprop tests with drying and wetting cycles (HYP);
- 1 shrinkage test (SSC).

The tests performed in stage 2 include:

- 1 unconsolidated undrained triaxial compression tests at natural water content (UU-n);
- 2 unconsolidated undrained triaxial compression test at dry condition (UU-d);
- 1 consolidated undrained triaxial compression test fully saturated (CU);
- 2 Hyprop tests with drying and wetting cycles (HYP);
- 1 shrinkage test (SSC).

To guarantee sufficient homogeneity of water content distribution within the sample during drying and wetting, the triaxial tests were conducted on 38 mm in diameter samples with a height to diameter ratio equal to 2.2. Preliminary comparison of TxCU results on 38-mm-diameter and 50-mm-diameter samples confirmed the absence of significant effects of the sample diameter on the stress–strain response of the material. The representative confining stress was set to 40 kPa in stage 1 and 15 kPa in stage 2. All the shear stages started from isotropic stress. As reported in Figure 2, for both tube 7 and tube 6 it was possible to obtain one undisturbed sample each due to the presence of sand.

Table 6. List of tests conducted on samples from borehole B002 at the Maasdijk near Oijen (stage 1)

Tube	Test ID	Sample ID	Water content	Portion	Averaged depth (m) NAP
8	UU-n	S1	Natural	Bottom	6.2
7	UU-d	S1	Dry	Bottom	6.5
8	UU-dw	S2	Drying – wetting	Mid	6.3
6	UU-n	S1	Natural	Mid	7.1
8	HYP	S3	Full saturation	Top	6.4
13	HYP	S1	Full saturation	Top	4.4
12	SSC	S1	Full saturation	Mid	4.7

Table 7. List of tests conducted on samples from borehole B002 at the Maasdijk near Oijen (stage 2)

Tube	Test ID	Sample ID	Water content	Portion	Averaged depth (m) NAP
1	UU-d	S1	Dry	Bottom	9.1
3	UU-d	S1	Dry	Top	8.4
4	UU-n	S1	Natural	Top	8.0
4	CU	S2	Full saturation	Bottom	7.9
2	HYP	S2	Full saturation	Mid	8.7
3	HYP	S2	Full saturation	Bottom	8.3
2	SSC	S3	Full saturation	Bottom	8.6

4.2. Results of the triaxial tests

Conventional triaxial stress – strain variables are used in presenting the results, namely deviatoric stress, q, and axial strain, ε_a. The data have been elaborated assuming a cross sectional area correction of equivalent cylinder and membrane correction has been applied to the radial stress as proposed by Fukushima & Tatsuoka (1984) and La Rochelle (1988). For samples showing a shear band, the stress – strain relationship is considered representative of the sample behaviour up to the maximum deviatoric stress. The results are presented for each stage.

Stage 1

Sample T7 S1 UU-d was first dried under controlled conditions, 17 °C and 73% relative humidity, for seven days before mounting it in the triaxial cell. Sample T8 S2 UU-dw was dried as sample T7 S1 UU-d. Afterwards, wetting was performed to re-establish the initial natural water content. The

sample was left resting over four days after wetting. The evolution of the water content for both samples is reported in Figure 19 and Figure 20.

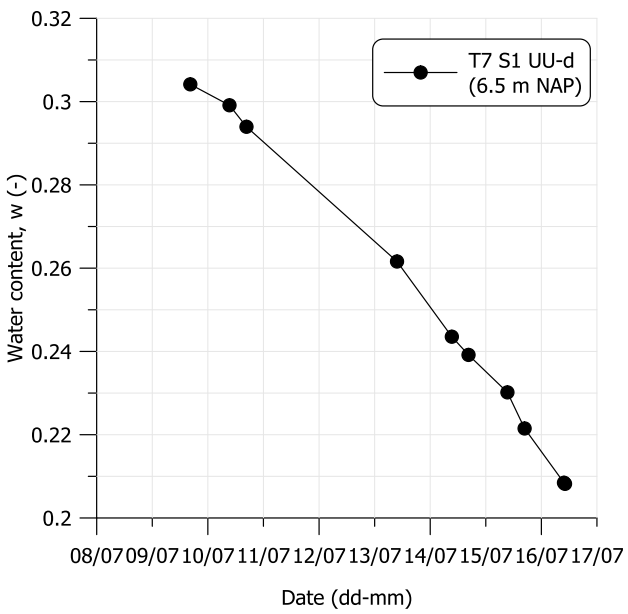

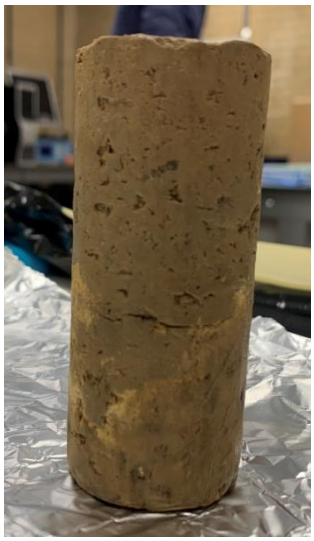

Figure 19. Drying stage on sample T7 S1 UU-d (picture at the end of the drying stage)

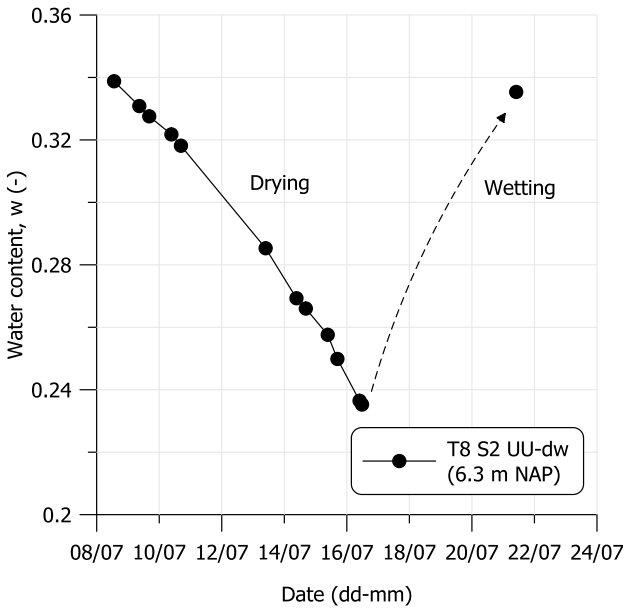

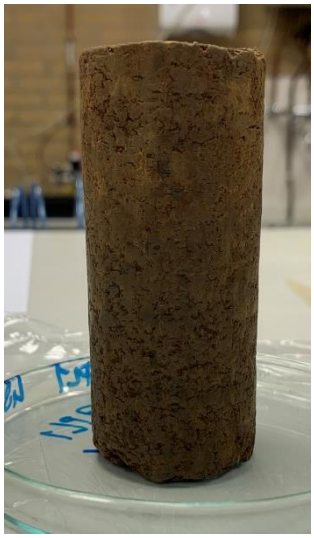

Figure 20. Drying and wetting stage on sample T8 S2 UU-dw (picture at the end of the drying stage)

The samples were then mounted in the triaxial apparatus. The index properties of the samples at the beginning of the triaxial tests are reported in Table 8. Sample T6 S1 UU-n obtained from tube 6 7.1 m NAP has a natural water content much lower than the other three samples. The material looks more sandy as confirmed by the Atterberg's limits. For the sake of clarity the test has been included in the following results.

Table 8. Index properties of the samples at the beginning of the triaxial tests (stage 1)

Sample ID	G_s (-)	w_{nat} (-)	w_0 (-)	S_{r0} (-)	w_p (-)	w_l (-)	OC (%)	σ_c (kPa)	Depth (m NAP)
T8 S1 UU-n	2.649	0.357	0.357	0.98	0.250	0.437	7.0	40	6.2
T7 S1 UU-d	2.674	0.304	0.208	0.81	0.208	0.345	4.2	40	6.5
T8 S2 UU-dw	2.658	0.339	0.335	0.97	0.246	0.404	5.6	40	6.3
T6 S1 UU-n	2.665	0.184	0.184	0.89	0.182	0.234	2.7	40	7.1

The particle size distribution for the four samples is displayed in Figure 21.

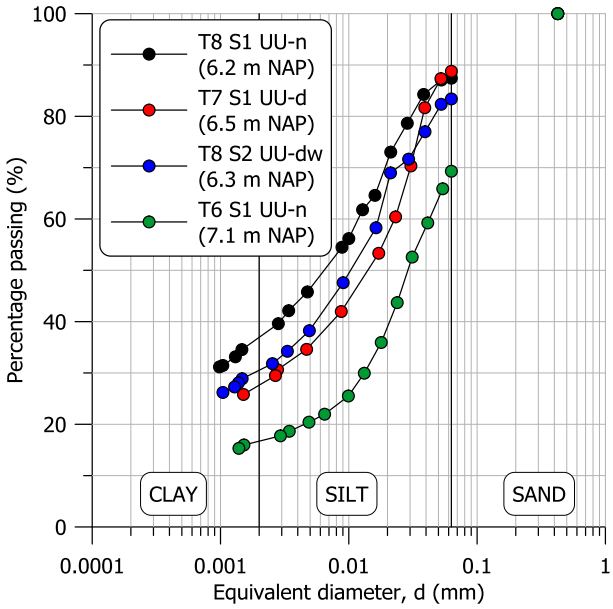

Figure 21. Particle size distribution for the four samples retrieved at depths 7.1, 6.5, 6.3, and 6.2 m NAP

The deviatoric stress - strain relationship for the four samples is compared in Figure 22. All the samples show a ductile asymptotic deviatoric response at failure. A barrel deformation mode was observed for all samples as shown in Figure 23. With reference to the three samples T8 S1 UU-n, T8 S2 UU-dw and T7 S1 UU-d, the comparison in Figure 22 shows a dramatic increase in the maximum deviatoric stress for sample T7 S1 UU-d tested after drying corresponding to a saturation degree equal to 0.81. At the end of the tests, each sample was cut in three parts for water content determination. The corresponding profiles are displayed in Figure 24.

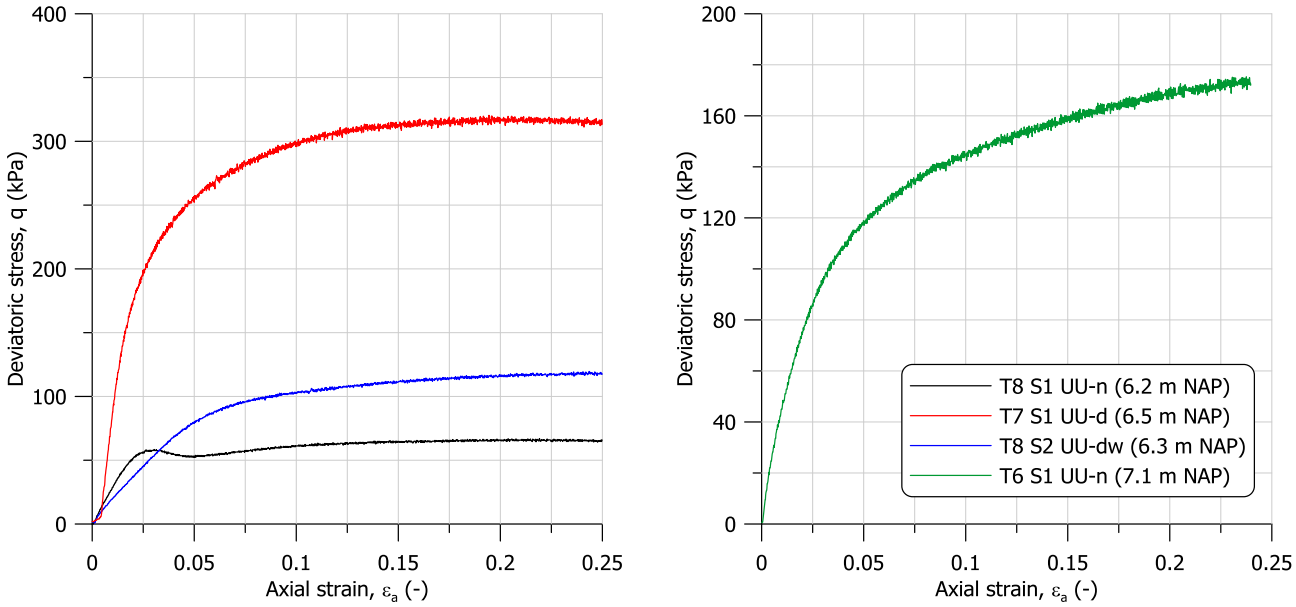

Figure 22. Deviatoric stress – strain relationship for the four samples retrieved at depths 7.1, 6.5, 6.3, and 6.2 m NAP

T8 S1 UU-n 6.2 m | T8 S2 UU-dw 6.3 m | T7 S1 UU-d 6.5 m | T6 S1 UU-n 7.1 m

Figure 23. Four samples retrieved at depths 7.1, 6.5, 6.3, and 6.2 m NAP at the end of the triaxial tests

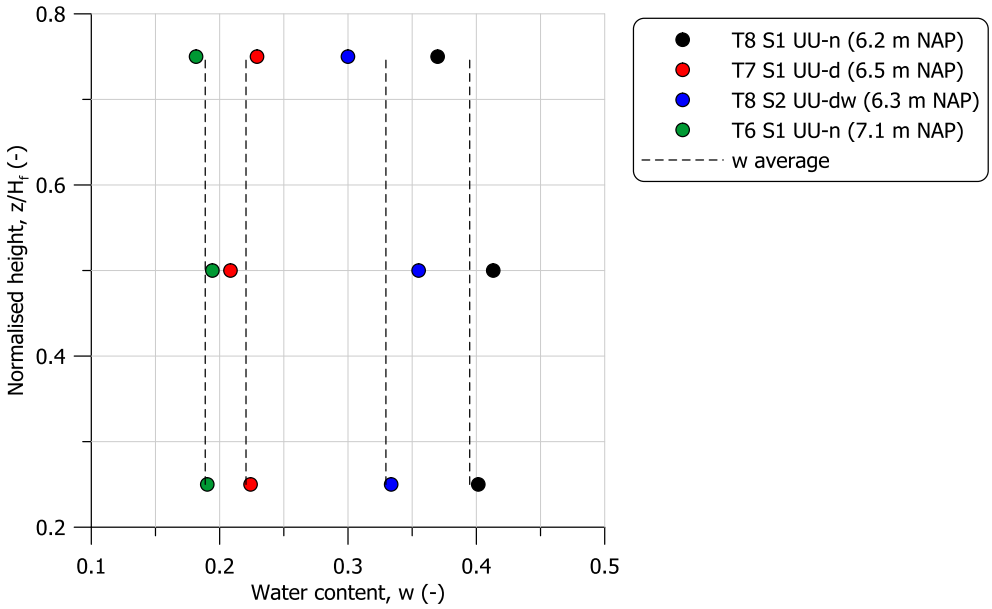

Figure 24. Water content profile at the end of the tests for the four samples retrieved at depths 7.1, 6.5, 6.3, and 6.2 m NAP

As displayed in Figure 24, the water content profile at the end of the tests can be considered relatively uniform. Higher water content was found in the central portion of the sample as a result of the barrelling deformation mode (Muraro & Jommi, 2019). The inherent variability of natural samples also contributed to the non-uniformity. It is worth noting that the water content at the end of the test on the sample T8 S1 UU-n was slightly higher than the initial one due to a small water intake. Therefore, the latter test can be considered representative of full saturation. The increase in the undrained shear strength at maximum deviatoric stress with decreasing water content is reported in Figure 25. Compared to fully saturated conditions, the undrained shear strength increases by a factor of about 4 for a degree of saturation 0.81.

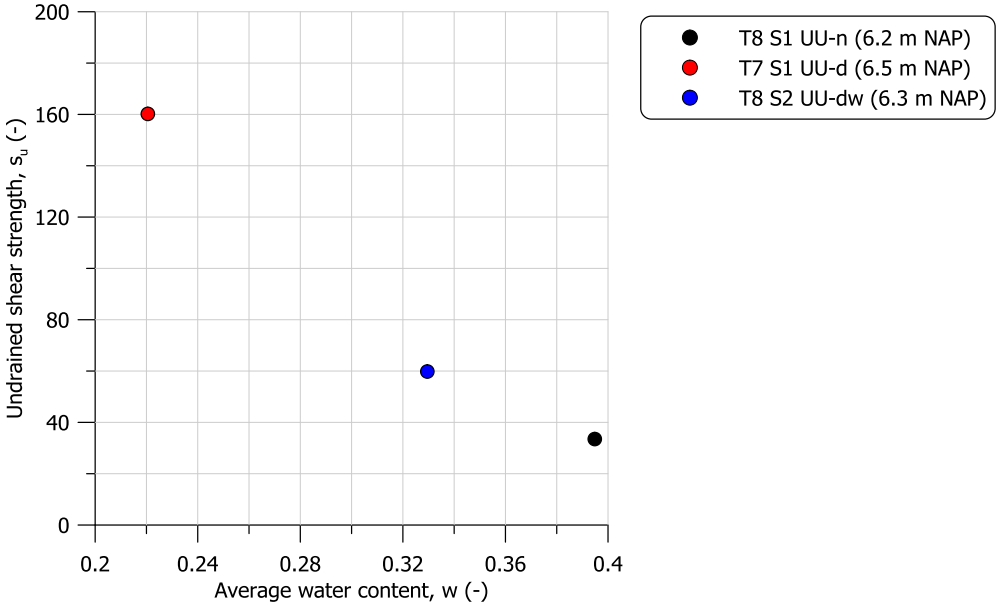

Figure 25. Undrained shear strength for the three samples retrieved at depths 6.5, 6.3, and 6.2 m NAP

Stage 2

Sample T1 S1 UU-d was first dried under controlled conditions, 17 °C and 70% relative humidity, for three days before mounting in the triaxial cell, while sample T3 S1 UU-d was dried for 6 days. The evolution of the water content is reported in Figure 26 and Figure 27. The samples were then mounted in the triaxial apparatus. The index properties of the samples at the beginning of the triaxial tests are reported in Table 9.

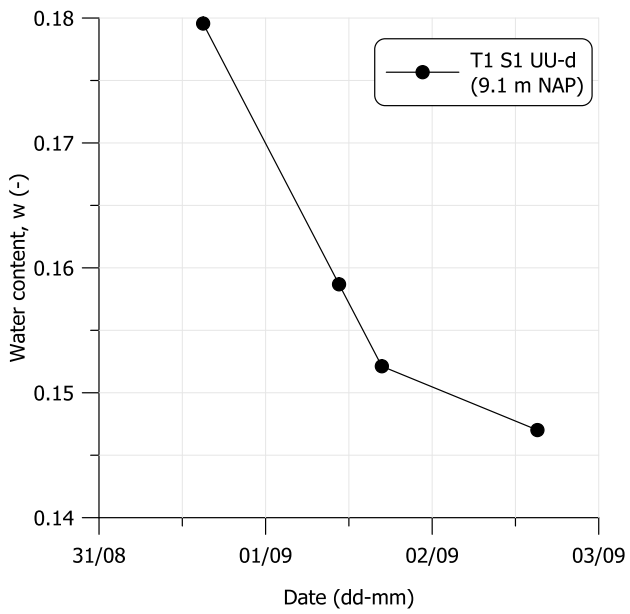

Figure 26. Drying stage on sample T1 S1 UU-d (picture at the end of the drying stage)

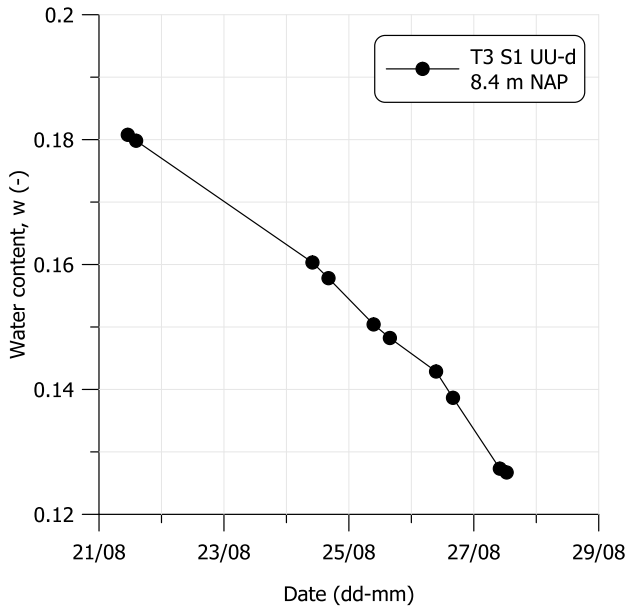

Figure 27. Drying stage on sample T3 S1 UU-d (picture at the end of the drying stage)

Table 9. Index properties of the samples at the beginning of the triaxial tests (stage 2)

Sample ID	G_s (-)	w_{nat} (-)	w_0 (-)	S_{r0} (-)	w_p (-)	w_l (-)	OC (%)	σ_c (kPa)	Depth (m NAP)
T1 S1 UU-d	2.603	0.180	0.145	0.57	0.213	0.332	4.6	15	9.1
T3 S1 UU-d	2.654	0.181	0.127	0.45	0.214	0.346	3.0	15	8.4
T4 S1 UU-n	2.642	0.186	0.186	0.67	0.215	0.339	4.0	15	8.0
T4 S2 CU	2.668	0.208	0.263	1.0	0.221	0.368	3.4	15*	7.9

*The sample T4 S2 CU was first saturated under back pressure 540 kPa and then isotropically consolidated to p'=15 kPa

The particle size distribution for the four samples is displayed in Figure 28.

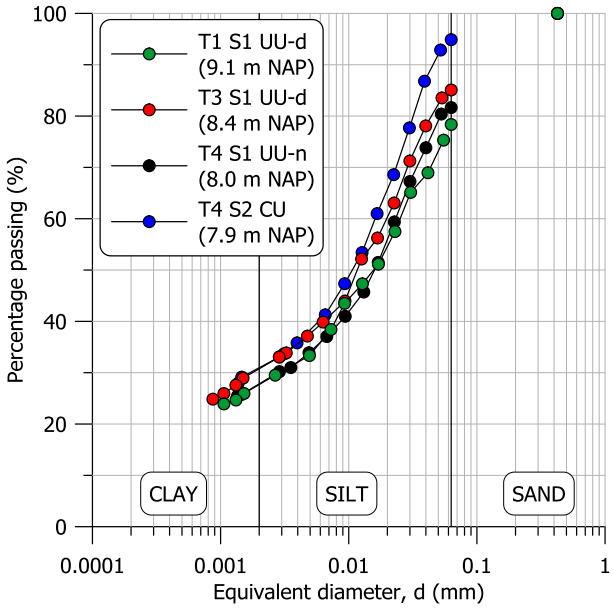

Figure 28. Particle size distribution for the four samples retrieved at depths 9.1, 8.4, 8.0, and 7.9 m NAP

The deviatoric stress strain relationship for the four samples is compared in Figure 29. Sample T4 S2 CU fully saturated showed a ductile asymptotic deviatoric response and a barrel deformation mode (Figure 30). On the contrary, the deviatoric response turned to be brittle as the degree of saturation decreased. The failure mode showed the formation of shear planes (samples T4 S1 UU-n and T1 S1 UU-d) and axial splitting (sample T3 S1 UU-d).

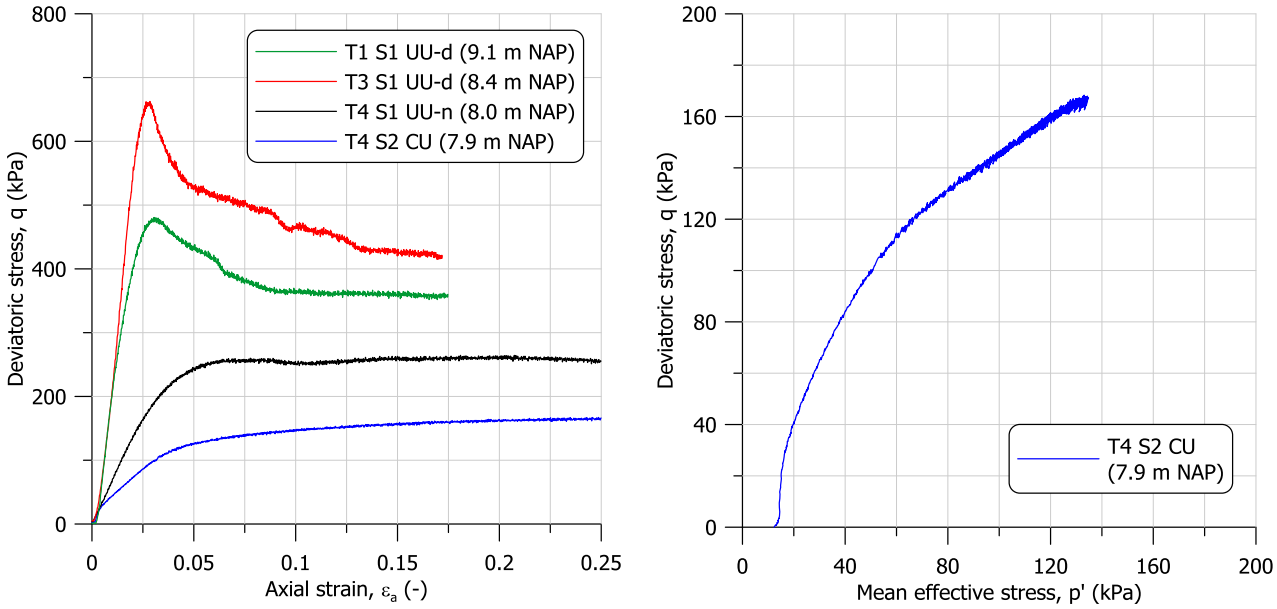

Figure 29. Deviatoric stress - strain relationship for the four samples retrieved at depths 9.1, 8.4, 8.0, and 7.9 m NAP and stress path for the sample T4 S2 CU

T1 S1 UU-d 9.1 m | T3 S1 UU-d 8.4 m | T4 S1 UU-n 8.0 m | T4 S2 CU 7.9 m

Figure 30. Four samples retrieved at depths 9.1, 8.4, 8.0, and 7.9 m NAP at the end of the triaxial tests

At the end of the tests, each sample was cut in three parts for water content determination. The corresponding profiles are displayed in Figure 31. As displayed, water content profile at the end of the tests can be considered relatively uniform.

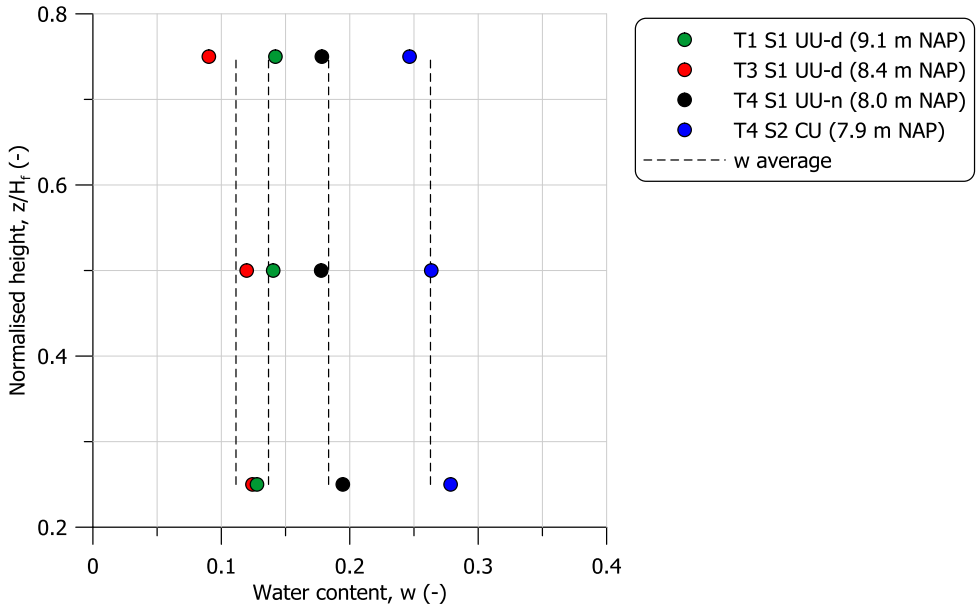

Figure 31. Water content profile at the end of the tests for the four samples retrieved at depths 9.1, 8.4, 8.0, and 7.9 m NAP

The increase in the undrained shear strength at maximum deviatoric stress with decreasing water content is reported in Figure 32. Compared to fully saturated conditions, the undrained shear strength increases by a factor of about 4 for a degree of saturation 0.45.

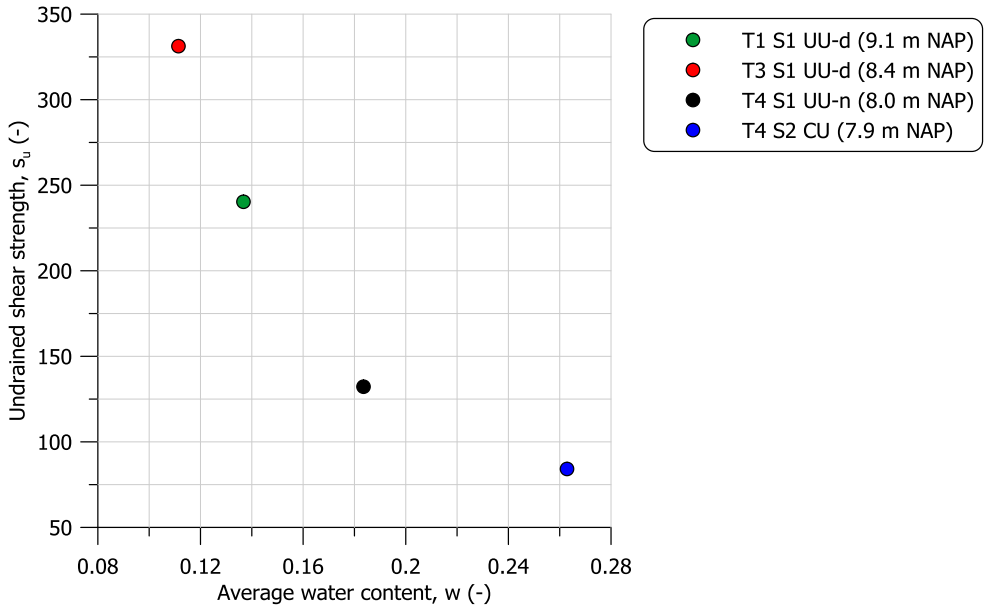

Figure 32. Undrained shear strength for the four samples retrieved at depths 9.1, 8.4, 8.0, and 7.9 m NAP

4.3. Results of the Hyprop tests

Stage 1

The retention properties of the soil have been investigated with the Hyprop device (Meter Group). One sample from Tube 8 and one from Tube 13 have been tested. As shown in Figure 2, Tube 7 (mid and top part) and Tube 6 contained mainly sand which hindered the possibility of performing further tests on undisturbed samples apart for the triaxial ones. For this reason, material from Tube 13 was used. Table 10 reports the main index properties of the samples at the beginning of the tests.

Table 10. Index properties of the samples at the beginning of the Hyprop tests (stage 1)

Tube	Sample ID	G_s (-)	w_0 (-)	Depth (m NAP)
8	T8 S3 HYP	2.689	0.341	6.4
13	T13 S1 HYP	2.687	0.289	4.5

The HYPROP consists of a main sensor unit comprising two tensiometers of different lengths. An 80 mm stainless steel ring with a 50mm height is used for containing the soil sample that is placed on the sensor unit (Figure 33). The entire setup sits on top of a weighing scale. The air-entry value of the ceramic tips is 880 kPa, but as the water in shaft cavitates earlier, the maximum suction that can be measured is approximately 100 kPa (Tollenaar et al., 2017). Due to the reduced sample diameter, 67 mm, a sequence of plastic - aluminium - plastic - aluminium film was placed on the later surface of the sample in order to avoid evaporation in the radial direction. Before installing the sample, a thin layer of slurry was placed at the bottom of the sensor base to avoid air entering.

Figure 33. Cross section of the Hyprop system® (User Manual Hyprop, 2015)

Cycles of drying and wetting were repeated, in order to draw the complete picture of the response. The results for sample T8 S3 HYP are displayed in Figure 34 and for the sample T13 S1 HYP in Figure 35. The data allow inferring the response of the soil (e.g. with a van Genuchten's model) for both drying and wetting events, which will facilitate the interpretation of the shear strength data, beyond their dependence on the water content, and hysteresis effects.

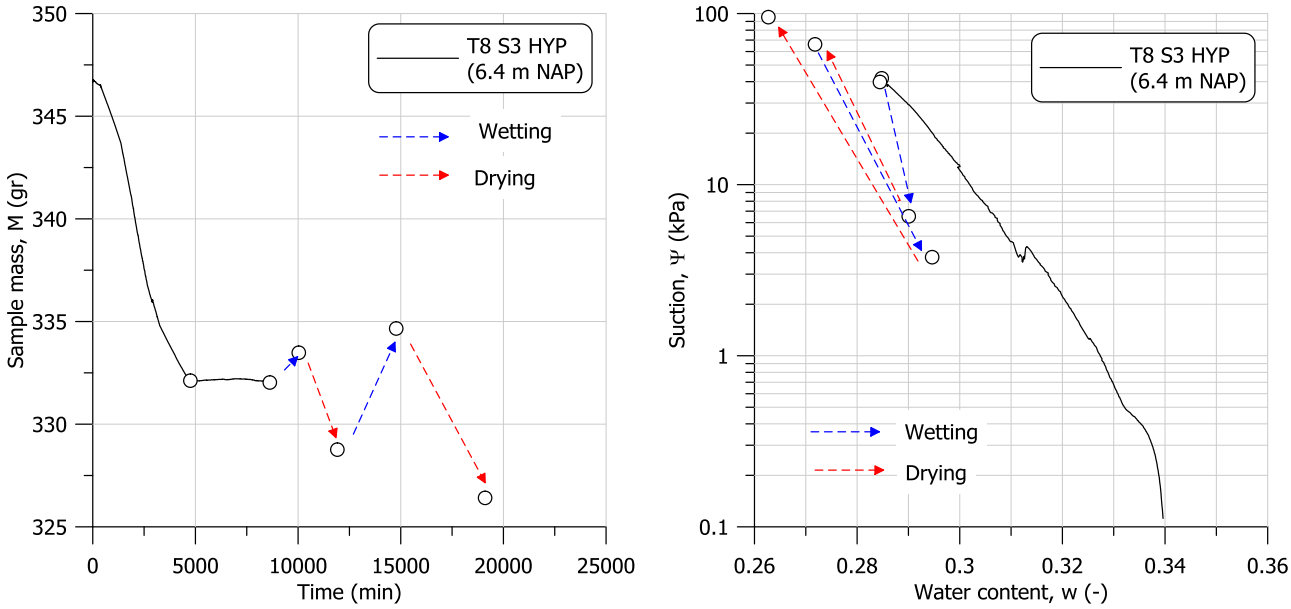

Figure 34. Results of the HYPROP test on sample T8 S3 HYP

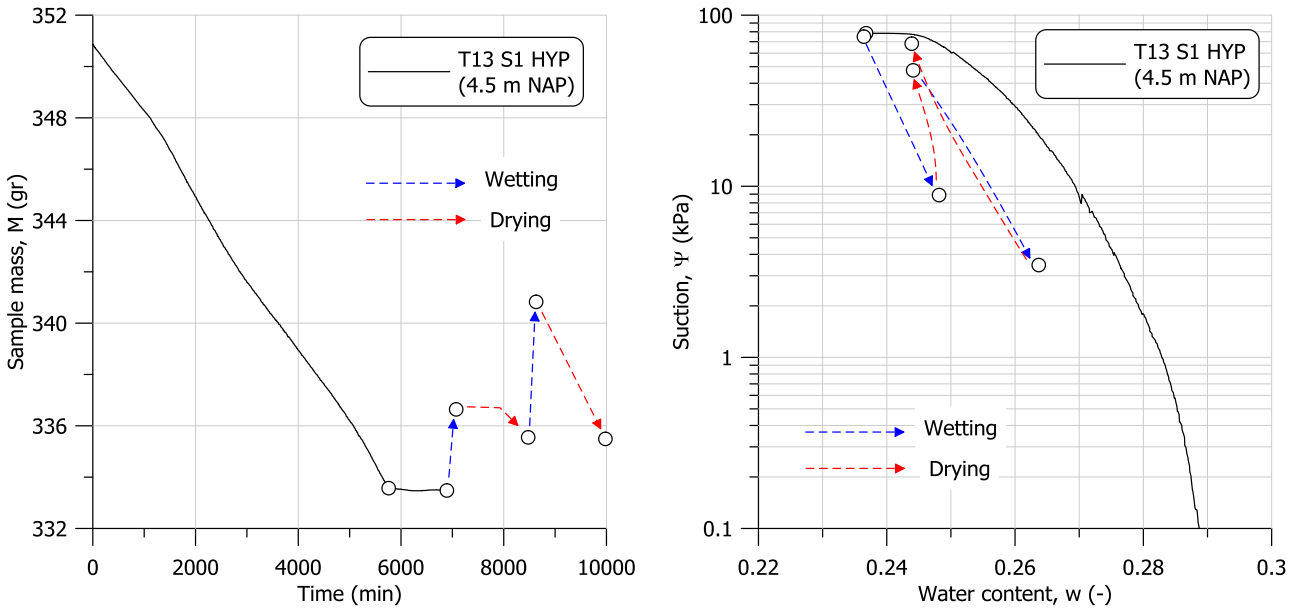

Figure 35. Results of the HYPROP test on sample T13 S1 HYP

Stage 2

The retention properties of the soil have been investigated with the Hyprop device (Meter Group). One sample from Tube 2 and one sample from Tube 3 have been tested. Table 11 reports the main index properties of the samples at the beginning of the tests. Cycles of drying and wetting were repeated, in order to draw the complete picture of the response. The results for sample T2 S2 HYP are displayed in Figure 36 and for the sample T3 S2 HYP in Figure 37. The data allow inferring the response of the soil (e.g. with a van Genuchten's model) for both drying and wetting events, which will facilitate the interpretation of the shear strength data, beyond their dependence on the water content, and hysteresis effects.

Table 11. Index properties of the samples at the beginning of the Hyprop tests (stage 2)

Tube	Sample ID	G_s (-)	w_0 (-)	Averaged depth (m) NAP
2	T2 S2 HYP	2.640	0.316	8.7
3	T3 S2 HYP	2.654	0.255	8.3

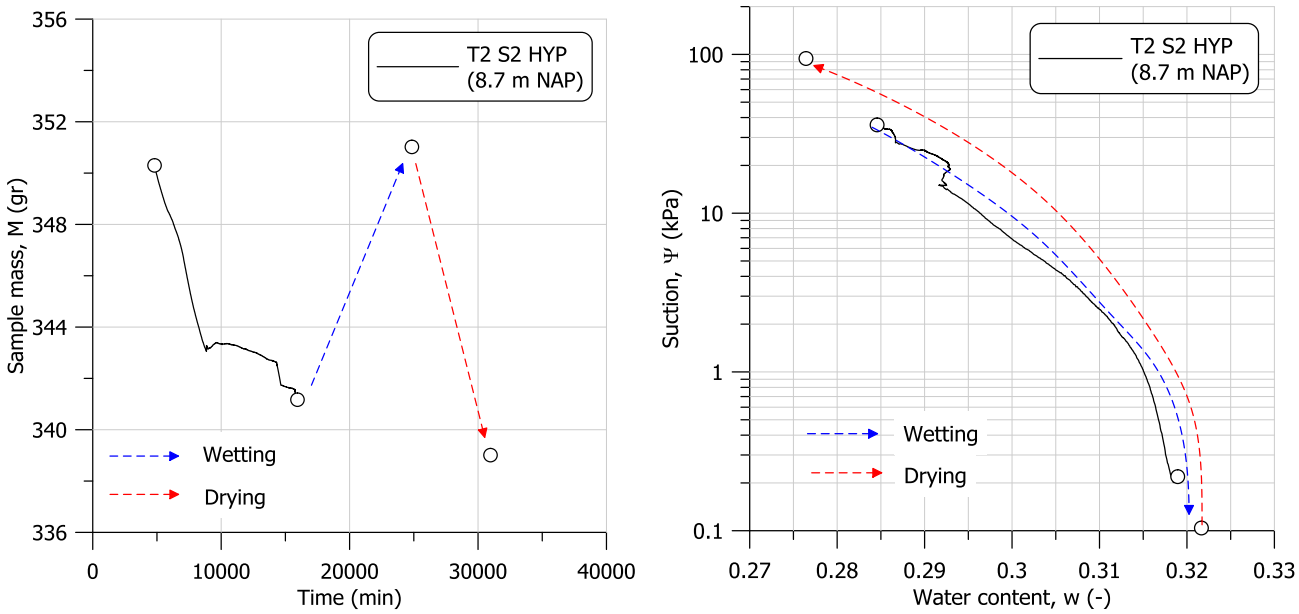

Figure 36. Results of the HYPROP test on sample T2 S2 HYP

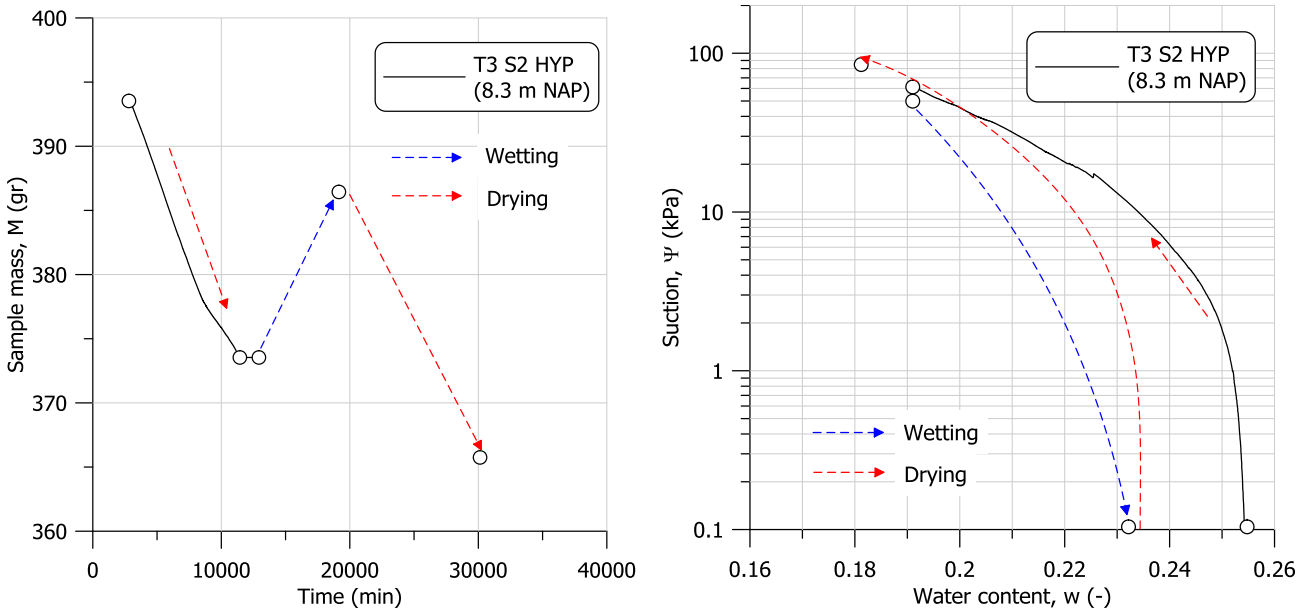

Figure 37. Results of the HYPROP test on sample T3 S2 HYP

4.4. Results of the shrinkage tests

Two shrinkage tests on samples T12 S1 SSC and T2 S3 SSC have been performed to complete the information on the retention properties. The samples, 38 mm in diameter and 38 mm in height were dried under controlled conditions, 17°C and 63% relative humidity, for several days. The sample mass and dimensions were measured at regular intervals during drying. Table 12 reports the main index properties of the samples at the beginning of the tests. The shrinkage curves for sample T12 S1 SSC and T2 S3 SSC are displayed in Figure 38 and Figure 39 in terms of void ratio, e, and water ratio, $e_w = wG_s$.

Table 12. Index properties of the samples at the beginning of the shrinkage test

Tube	Sample ID	G_s (-)	w_0 (-)	Averaged depth (m) NAP
12	T12 S1 SSC	2.674	0.332	4.7
2	T2 S3 SSC	2.661	0.330	8.6

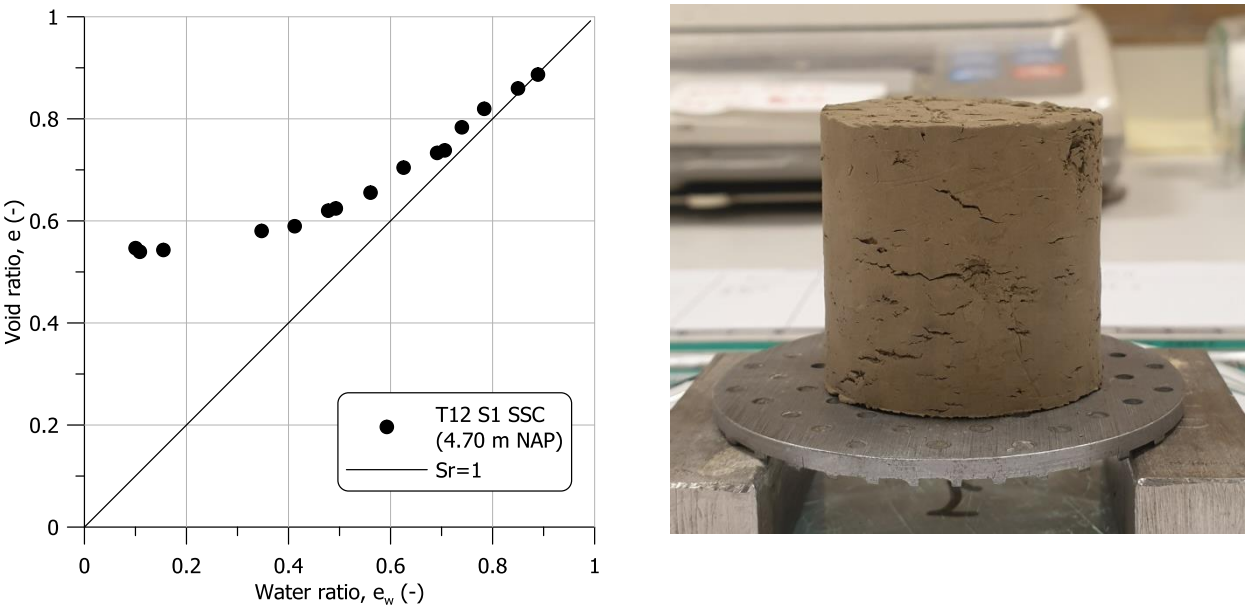

Figure 38. Results of the shrinkage test on sample T12 S1 SSC

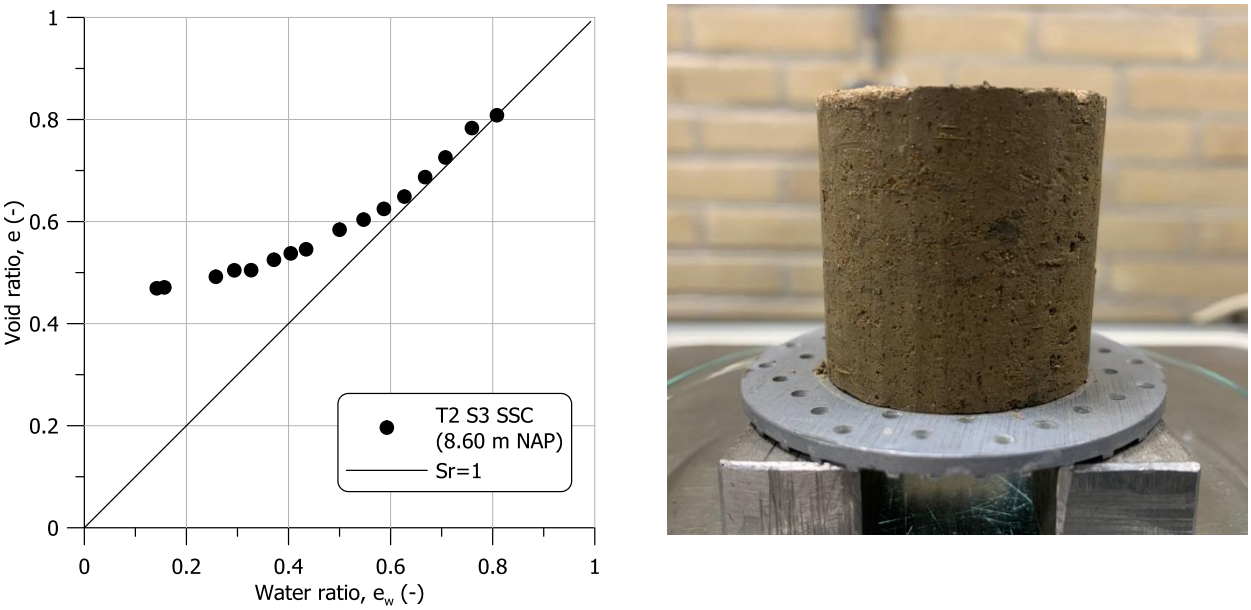

Figure 39. Results of the shrinkage test on sample T2 S3 SSC

5. LABORATORY TESTS AT THE IJSSELDIJK NEAR WESTERVOORT

5.1. Introduction

The laboratory tests are conducted on undisturbed samples from the borehole B202 retrieved on 11/08/2020 in the dry period. Samples from two depths are tested in subsequent investigation stages. Over stage 1, the soil between 8.5 m and 9.2 m NAP is tested (Tube 4, 5), while the stage 2 includes tests on samples between 9.3 m and 10.1 m NAP (Tube 1, 2, 3). In the following the results collected during stage 1 and stage 2 are presented (Table 13 and Table 14 respectively).
The tests performed in stage 1 include:

- 1 consolidated undrained triaxial compression test fully saturated (CU);
- 1 unconsolidated undrained triaxial compression test at dry condition (UU-d);
- 2 unconsolidated undrained triaxial compression test on a sample after drying and wetting cycle (UU-dw);
- 2 Hyprop tests with drying and wetting cycles (HYP);
- 1 shrinkage test (SSC).

The tests performed in stage 2 include:

- 1 consolidated undrained triaxial compression test fully saturated (CU);
- 2 unconsolidated undrained triaxial compression tests at natural water content (UU-n);
- 1 unconsolidated undrained triaxial compression test at dry condition (UU-d);
- 2 Hyprop tests with drying and wetting cycles (HYP);
- 1 shrinkage test (SSC).

To guarantee sufficient homogeneity of water content distribution within the sample during drying and wetting, the triaxial tests were conducted on 38 mm in diameter samples with a height to diameter ratio equal to 2.2. The representative confining stress was set to 10 kPa in both stage 1 stage 2 considering the proximity of the tubes investigated and the reduced amount of soil available for the investigation. All the shear stages started from isotropic stress.

Table 13. List of tests conducted on samples from borehole B202 at the Ijsseldijk near Westervoort (stage 1)

Tube	Test ID	Sample ID	Water content	Portion	Averaged depth (m) NAP
4	CU	S1	Full saturation	Bottom	8.85
4	UU-d	S2	Dry	Mid	8.95
4	UU-dw	S3	Drying – wetting	Top	9.05
5	UU-dw	S1	Drying – wetting	Mid	8.65
4	HYP	S4	Full saturation	Top	9.10
5	HYP	S2	Full saturation	Top	8.75
5	SSC	S3	Full saturation	Mid	8.60

Table 14. List of tests conducted on samples from borehole B202 at the Ijsseldijk near Westervoort (stage 2)

Tube	Test ID	Sample ID	Water content	Portion	Averaged depth (m) NAP
3	CU	S1	Full saturation	Mid	9.45
3	UU-n	S2	Natural	Bottom	9.30
2	UU-d	S1	Dry	Bottom	9.75
1	UU-n	S1	Natural	Bottom	10.05
3	HYP	S3	Full saturation	Top	9.55
2	HYP	S2	Full saturation	Mid	9.85
3	SSC	S4	Full saturation	Top	9.50

5.2. Results of the triaxial tests

Conventional triaxial stress – strain variables are used in presenting the results, namely deviatoric stress, q, and axial strain, ε_a. The data have been elaborated assuming a cross sectional area correction of equivalent cylinder and membrane correction has been applied to the radial stress as proposed by Fukushima & Tatsuoka (1984) and La Rochelle (1988). For samples showing a shear band, the stress – strain relationship is considered representative of the sample behaviour up to the maximum deviatoric stress. The results are presented for each stage.

Stage 1

Sample T4 S2 UU-d was dried under controlled conditions, 17 °C and 73% relative humidity, for five days before mounting in the triaxial cell. Sample T4 S3 UU-dw and sample T5 S1 UU-dw were first dried for three and nine days respectively. Afterwards, wetting at the target water content was performed and the samples were left resting over four days before mounting them in the triaxial apparatus. The evolution of the water content for all the three samples is reported in Figure 40, Figure 41, and Figure 42.

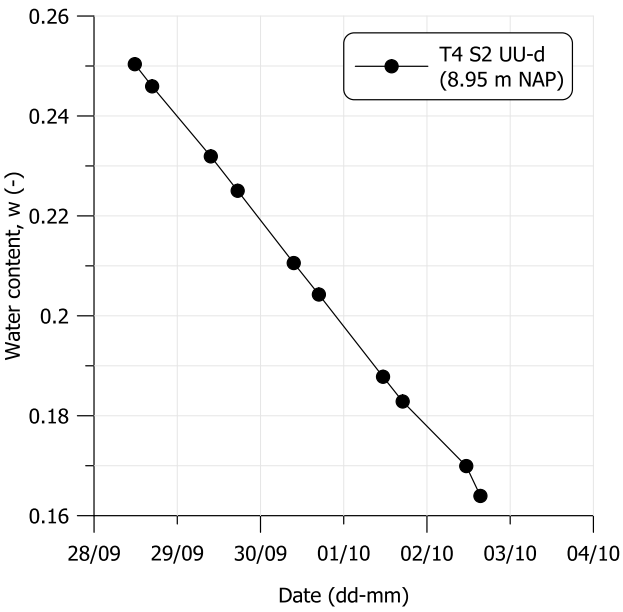

Figure 40. Drying stage on sample T4 S2 UU-d (picture at the end of the drying stage)

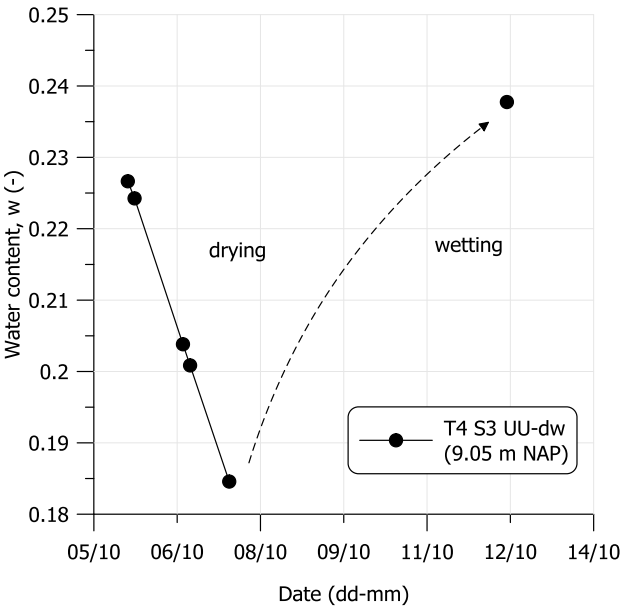

Figure 41. Drying and wetting stage on sample T4 S3 UU-dw (picture at the end of the drying stage)

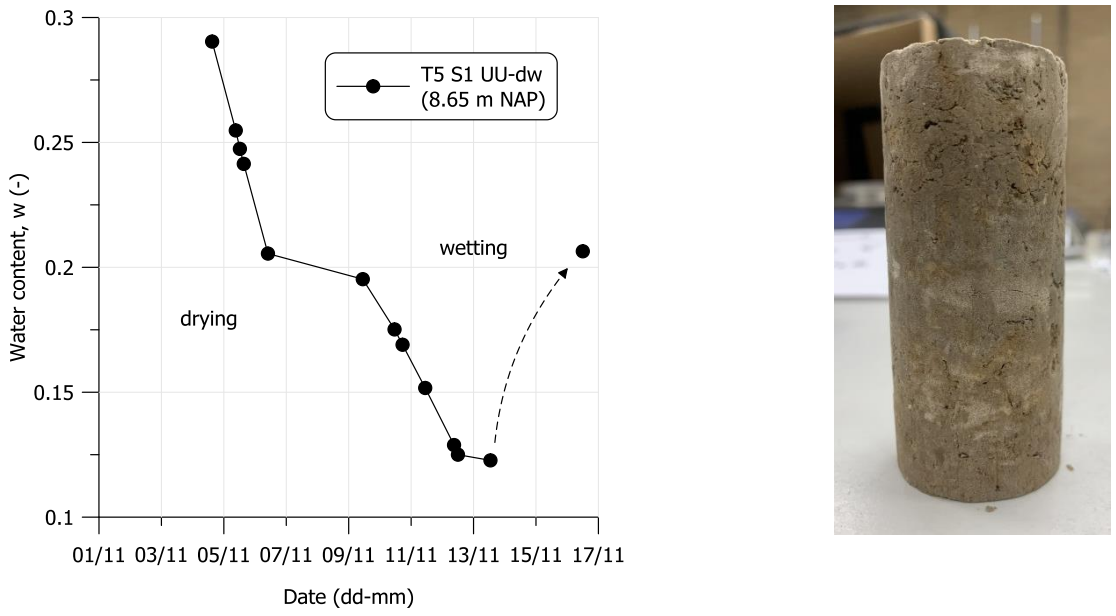

Figure 42. Drying and wetting stage on sample T5 S1 UU-dw (picture at the end of the drying stage)

The index properties of the samples at the beginning of the triaxial tests are reported in Table 15.

Table 15. Index properties of the samples at the beginning of the triaxial tests (stage 1)

Sample ID	G_s (-)	w_{nat} (-)	w_0 (-)	S_{r0} (-)	w_p (-)	w_l (-)	OC (%)	σ_c (kPa)	z (m NAP)
T4 S1 CU	2.678	0.259	0.278	1.0	0.211	0.329	1.6	10*	8.85
T4 S2 UU-d	2.688	0.250	0.164	0.67	0.206	0.319	1.9	10	8.95
T4 S3 UU-dw	2.652	0.227	0.238	0.94	0.203	0.296	1.7	10	9.05
T5 S1 UU-dw	2.681	0.290	0.202	0.72	0.209	0.321	1.4	10	8.65

*The sample T4 S1 CU was first saturated under back pressure 395 kPa and then isotropically consolidated to p'=10 kPa

The particle size distribution for the four samples is displayed in Figure 43.

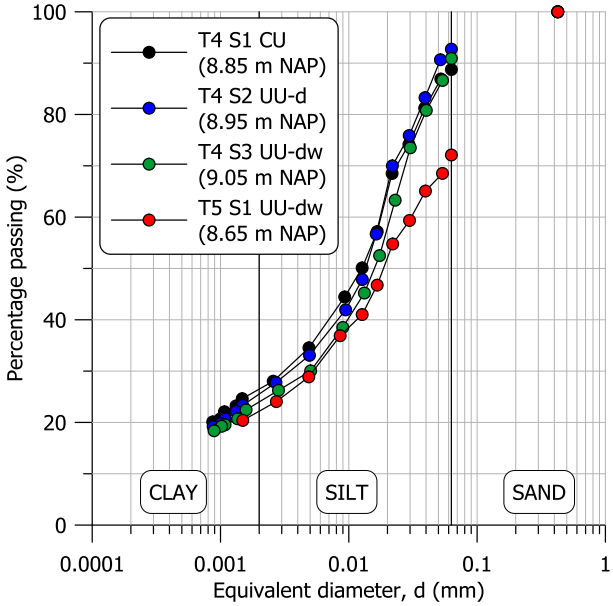

Figure 43. Particle size distribution for the four samples retrieved at depths 9.05, 8.95, 8.85, and 8.65 m NAP

The deviatoric stress - strain relationship for the four samples is compared in Figure 44. The comparison shows a dramatic increase in the maximum deviatoric stress for sample T4 S2 UU-d tested after drying corresponding to a saturation degree equal to 0.67 accompanied by a brittle failure mode (Figure 45). At the end of the tests, each sample was cut in three parts for water content determination. The corresponding profiles are displayed in Figure 46.

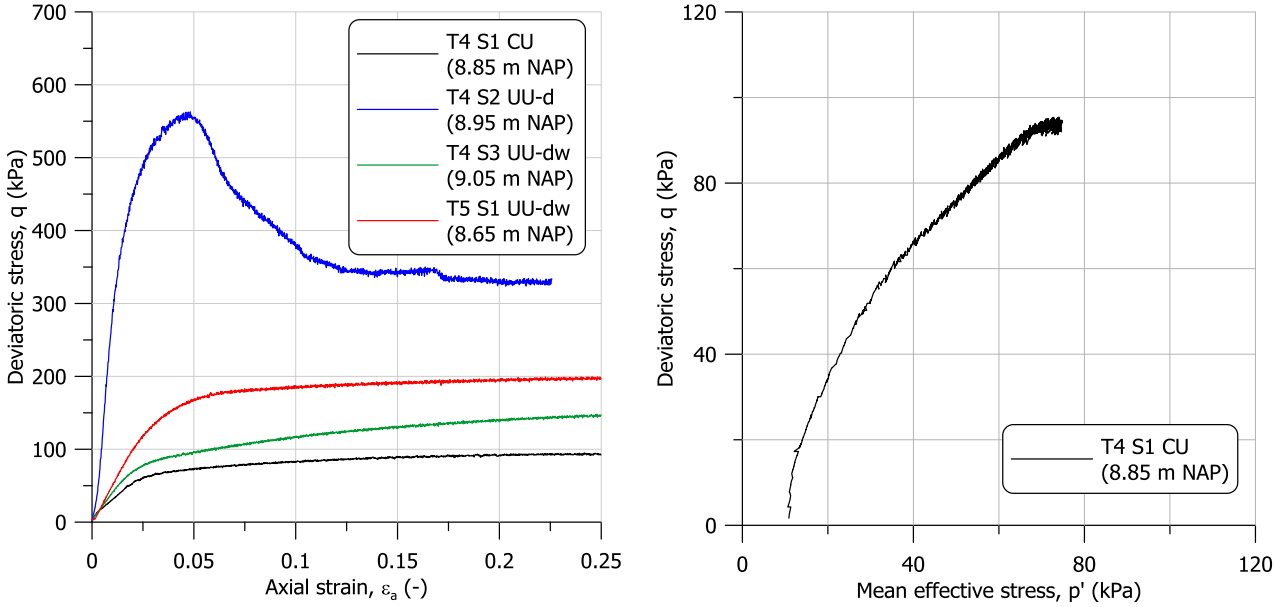

Figure 44. Deviatoric stress – strain relationship for the four samples retrieved at depths 9.05, 8.95, 8.85, and 8.65 m NAP and stress path for the sample T4 S1 CU

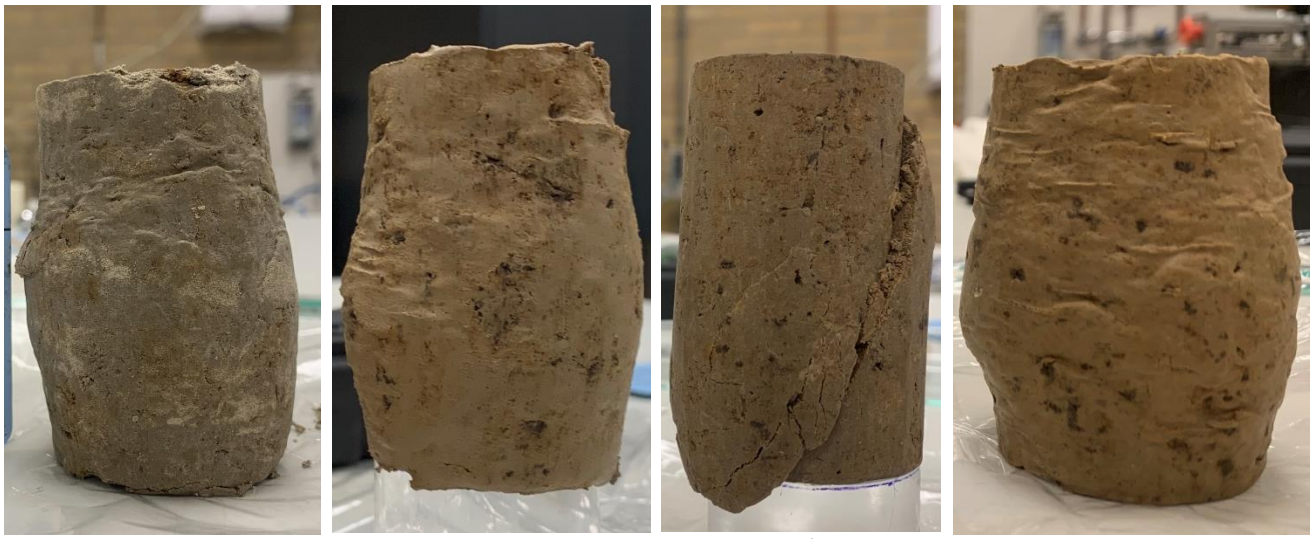

Figure 45. Four samples retrieved at depths 9.05, 8.95, 8.85, and 8.65 m NAP at the end of the triaxial tests

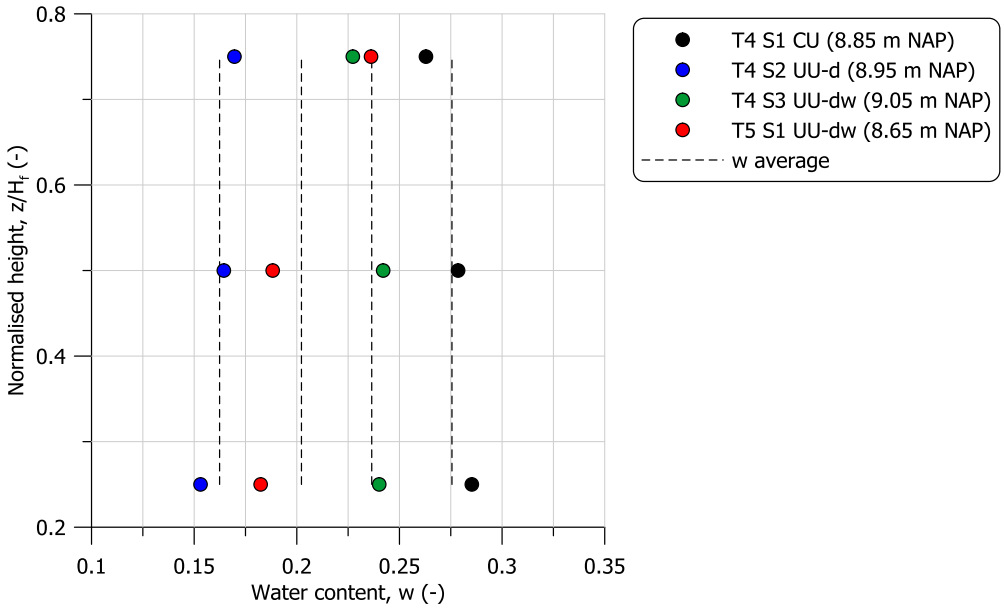

Figure 46. Water content profile at the end of the tests for the four samples retrieved at depths 9.05, 8.95, 8.85, and 8.65 m NAP

As displayed in Figure 46, the profile of water content at the end of the tests can be considered relatively uniform. The inherent variability of natural samples also contributed to the non-uniformity. Only the sample T5 S1 UU-dw showed a much higher water content at the top. The inspection at the end of the test revealed the presence of a sand core in the upper part of the sample. The deformation mode reported in Figure 45 also resembles this clear non-homogeneity. The particle size distribution reported in Figure 43 confirmed a higher percentage of sand. The increase in the undrained shear strength at maximum deviatoric stress with decreasing water content is reported in Figure 47. Compared to fully saturated conditions, the undrained shear strength increases by a factor of about 5 for a degree of saturation 0.67.

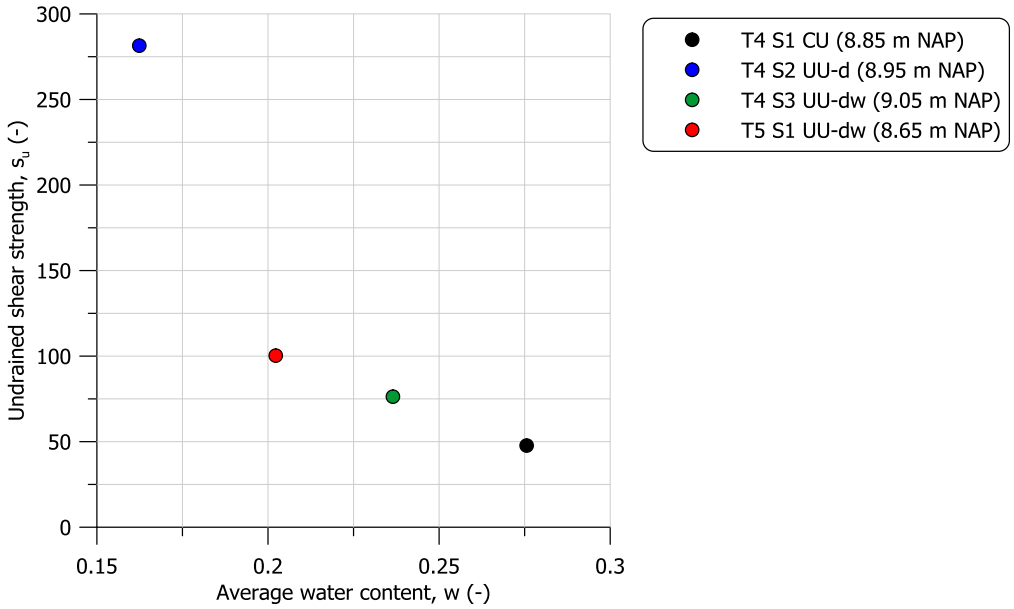

Figure 47. Undrained shear strength for the four samples retrieved at depths 9.05, 8.95, 8.85, and 8.65 m NAP

Stage 2

Sample T2 S1 UU-d was first dried under controlled conditions, 17 °C and 73% relative humidity, for one day before mounting in the triaxial cell. The evolution of the water content is reported in Figure 48.

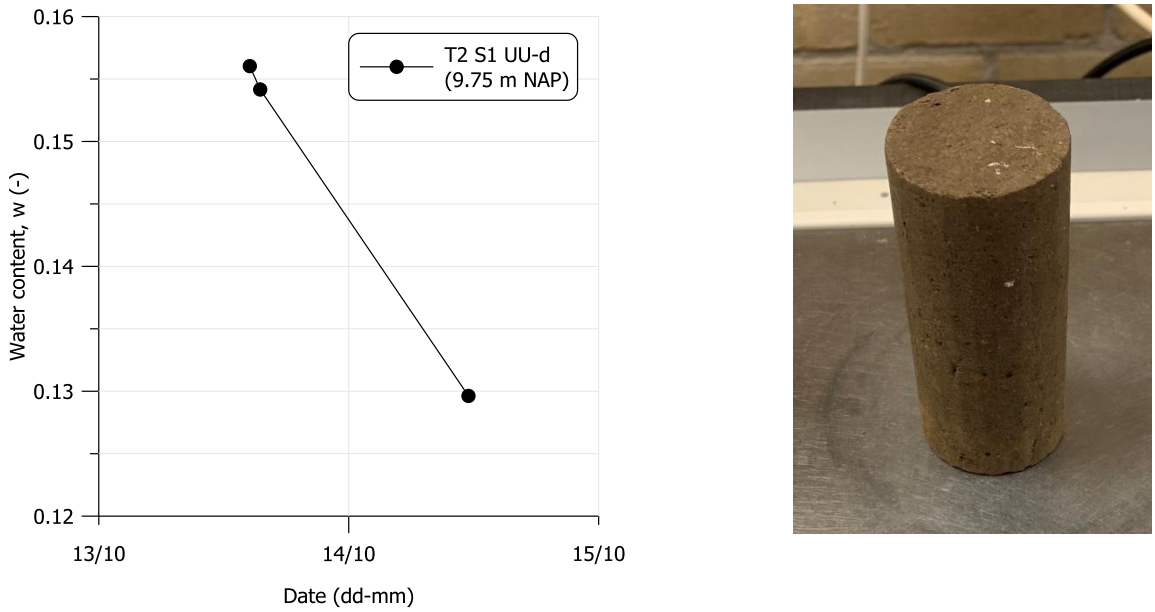

Figure 48. Drying stage on sample T2 S1 UU-d (picture at the end of the drying stage)

The index properties of the samples at the beginning of the triaxial tests are reported in Table 16.

Table 16. Index properties of the samples at the beginning of the triaxial tests (stage 2)

Sample ID	G_s (-)	w_{nat} (-)	w_0 (-)	S_{r0} (-)	w_p (-)	w_l (-)	OC (%)	σ_c (kPa)	z (m NAP)
T3 S1 CU	2.669	0.192	0.267	1.0	0.193	0.261	1.6	10*	9.45
T3 S2 UU-n	2.674	0.188	0.188	0.79	0.201	0.260	1.5	10	9.30
T2 S1 UU-d	2.636	0.156	0.130	0.64	0.189	0.244	2.6	10	9.75
T1 S1 UU-n	2.674	0.077	0.077	0.37	0.199	0.266	2.4	10	10.05

*The sample T3 S1 CU was first saturated under back pressure 500 kPa and then isotropically consolidated to p'=10 kPa

The particle size distribution for the four samples is displayed in Figure 49.

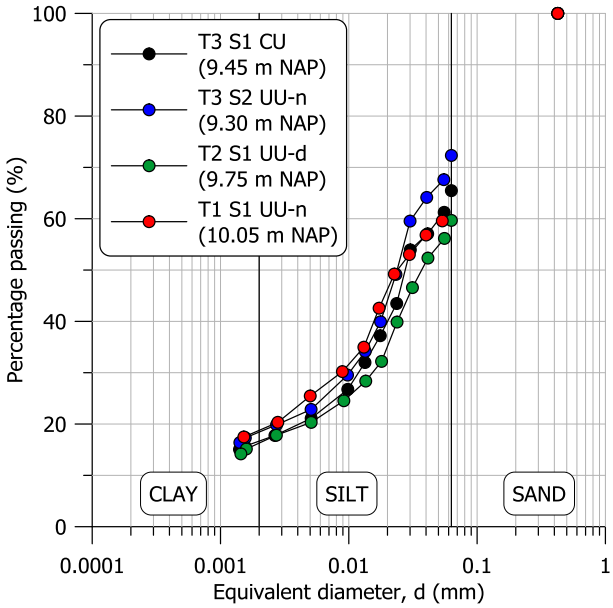

Figure 49. Particle size distribution for the four samples retrieved at depths 10.05, 9.75, 9.45, and 9.3 m NAP

The deviatoric stress - strain relationship for the four samples is compared in Figure 50. The comparison shows a dramatic increase in the maximum deviatoric stress for sample T2 S1 UU-d tested after drying corresponding to a saturation degree equal to 0.64 accompanied by a brittle failure mode (Figure 51). The same consideration holds for the sample T1 S1 UU-n tested at the natural water content corresponding to a saturation degree of about 0.37. At the end of the tests, each sample was cut in three parts for water content determination. The corresponding profiles are displayed in Figure 52.

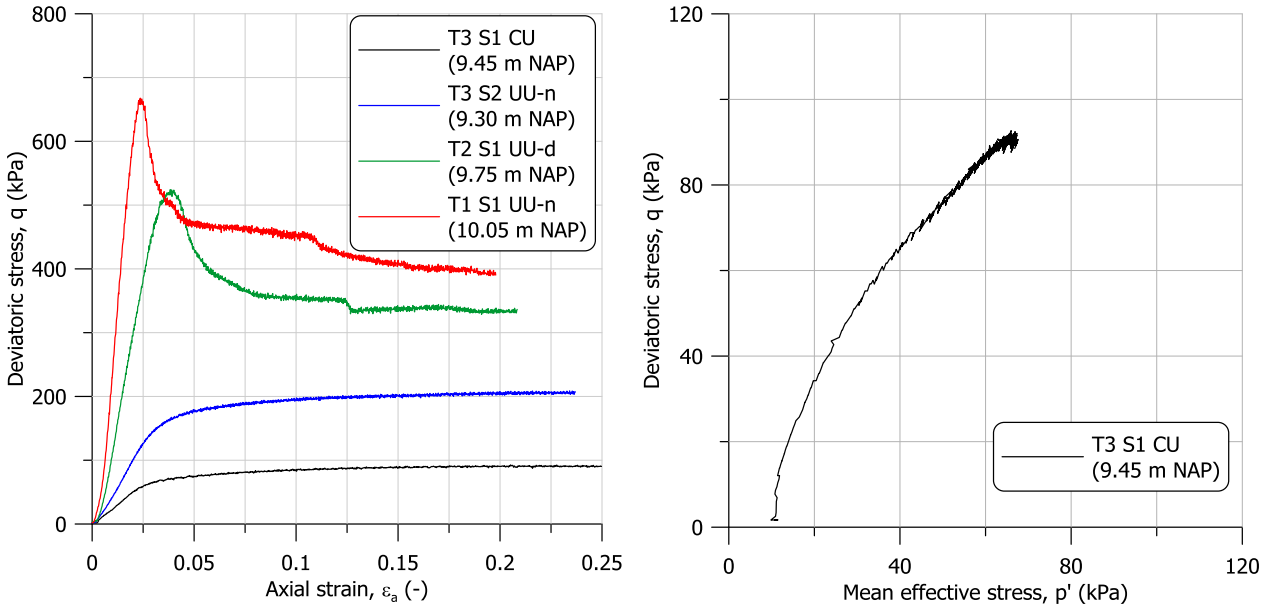

Figure 50. Deviatoric stress – strain relationship for the four samples retrieved at depths 10.05, 9.75, 9.45, and 9.3 m NAP and stress path for the sample T3 S1 CU

T3 S1 CU 9.45 m | T3 S2 UU-d 9.30 m | T2 S1 UU-d 9.75 m | T1 S1 UU-n 10.05 m

Figure 51. Four samples retrieved at depths 10.05, 9.75, 9.45, and 9.3 m NAP at the end of the triaxial tests

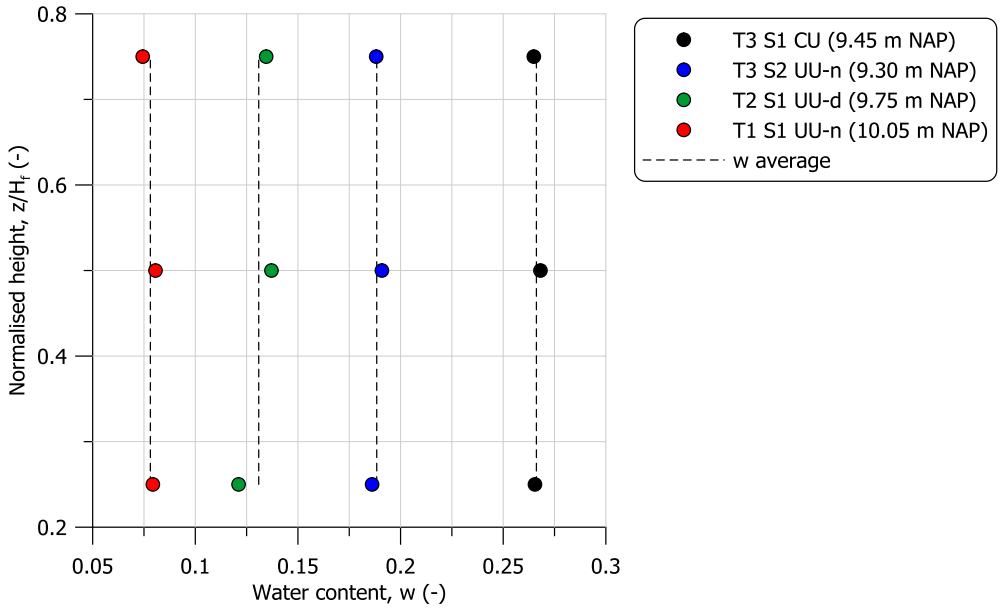

Figure 52. Water content profile at the end of the tests for the four samples retrieved at depths 10.05, 9.75, 9.45, and 9.3 m NAP

As displayed in Figure 52, the profile of water content at the end of the tests can be considered relatively uniform. The inherent variability of natural samples also contributed to the non-uniformity. The increase in the undrained shear strength at maximum deviatoric stress with decreasing water content is reported in Figure 53. Compared to fully saturated conditions, the undrained shear strength increases by a factor of about 6 for a degree of saturation 0.37.

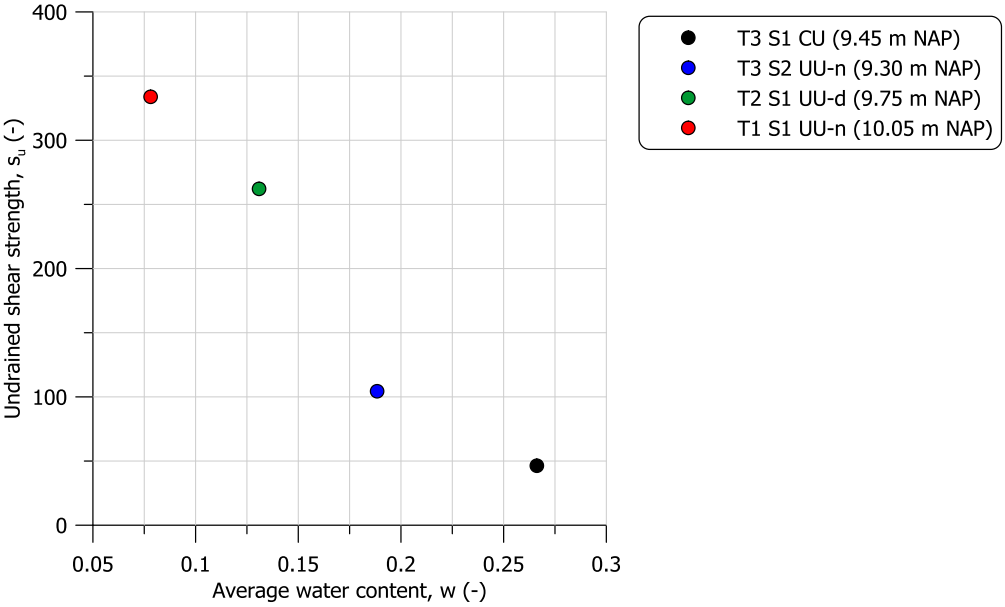

Figure 53. Undrained shear strength for the four samples retrieved at depths 10.05, 9.75, 9.45, and 9.3 m NAP

5.3. Results of the Hyprop tests

Stage 1

The retention properties of the soil have been investigated with the Hyprop device (Meter Group). One sample from Tube 4 and one from Tube 5 have been tested. Table 17 reports the main index properties of the samples at the beginning of the tests. Cycles of drying and wetting were repeated, in order to draw the complete picture of the response. The results for sample T4 S4 HYP and T5 S2 HYP are displayed in Figure 54 and Figure 55. The data allow inferring the response of the soil (e.g. with a van Genuchten's model) for both drying and wetting events, which will facilitate the interpretation of the shear strength data, beyond their dependence on the water content, and hysteresis effects.

Table 17. Index properties of the samples at the beginning of the Hyprop tests (stage 1)

Tube	Sample ID	G_s (-)	w_0 (-)	Averaged depth (m) NAP
4	T4 S4 HYP	2.652	0.265	9.10
5	T5 S2 HYP	2.678	0.301	8.75

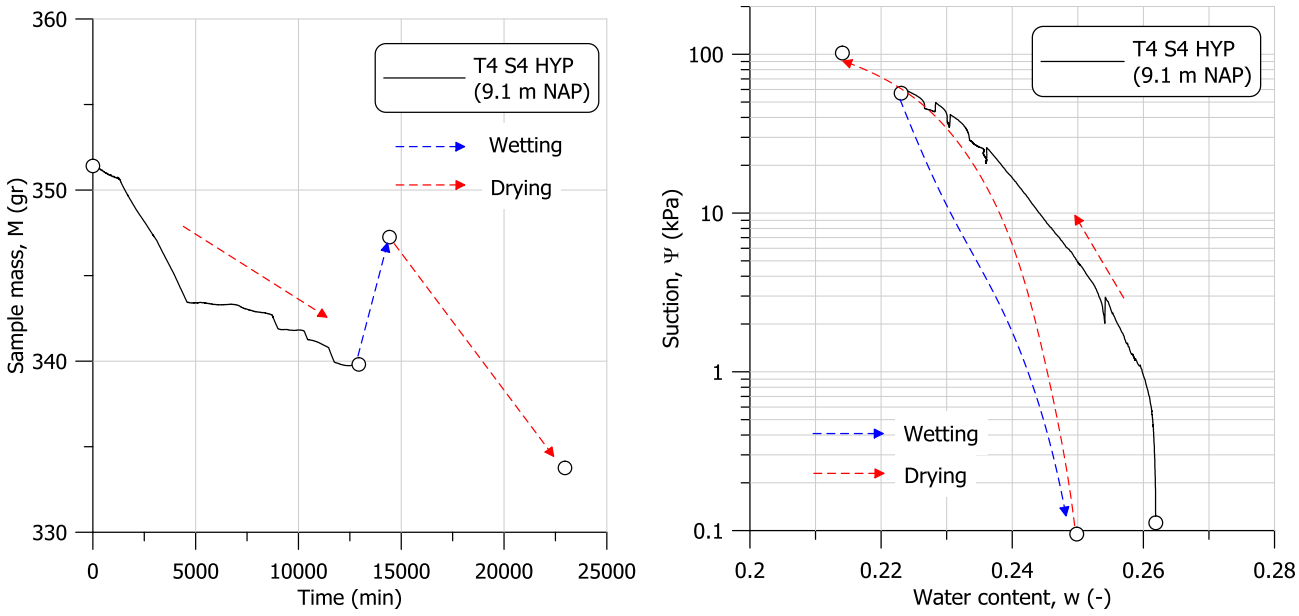

Figure 54. Results of the HYPROP test on sample T4 S4 HYP

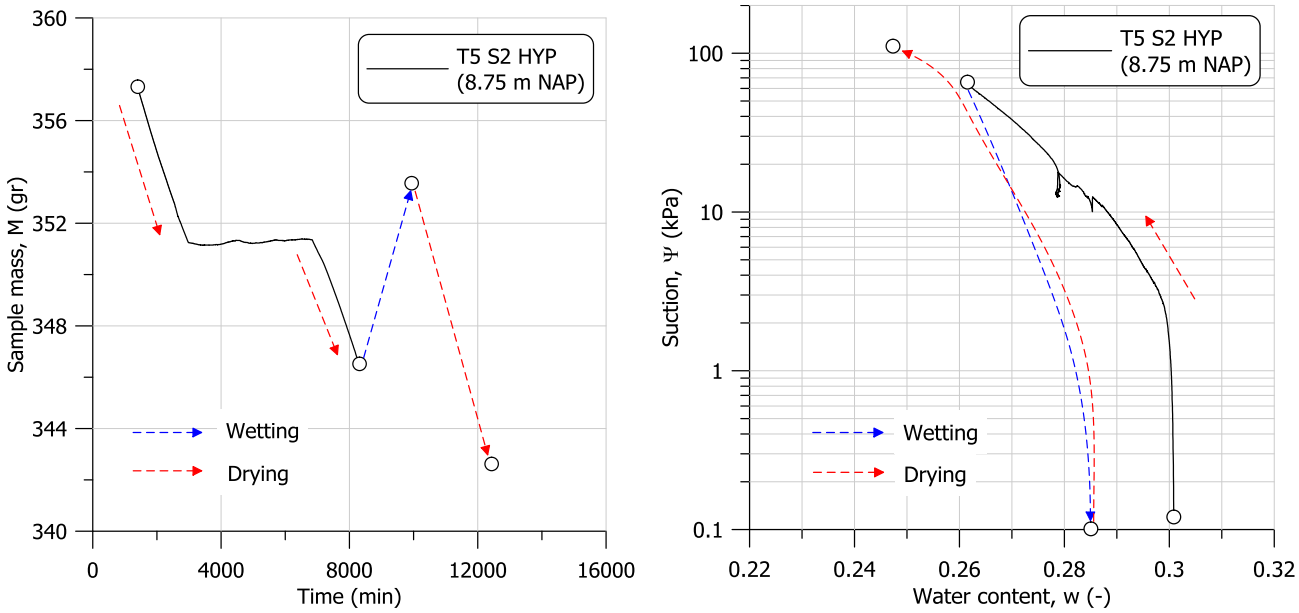

Figure 55. Results of the HYPROP test on sample T5 S2 HYP

Stage 2

The retention properties of the soil have been investigated with the Hyprop device (Meter Group). One sample from Tube 3 and one from Tube 2 have been tested. Table 18 reports the main index properties of the samples at the beginning of the tests. Cycles of drying and wetting were repeated, in order to draw the complete picture of the response. The results for sample T3 S3 HYP and T2 S2 HYP are displayed in Figure 56 and Figure 57. The data allow inferring the response of the soil (e.g. with a van Genuchten's model) for both drying and wetting events, which will facilitate the interpretation of the shear strength data, beyond their dependence on the water content, and hysteresis effects.

Table 18. Index properties of the samples at the beginning of the Hyprop tests (stage 2)

Tube	Sample ID	G_s (-)	w_0 (-)	Averaged depth (m) NAP
3	T3 S3 HYP	2.669	0.255	9.55
2	T2 S2 HYP	2.636	0.239	9.85

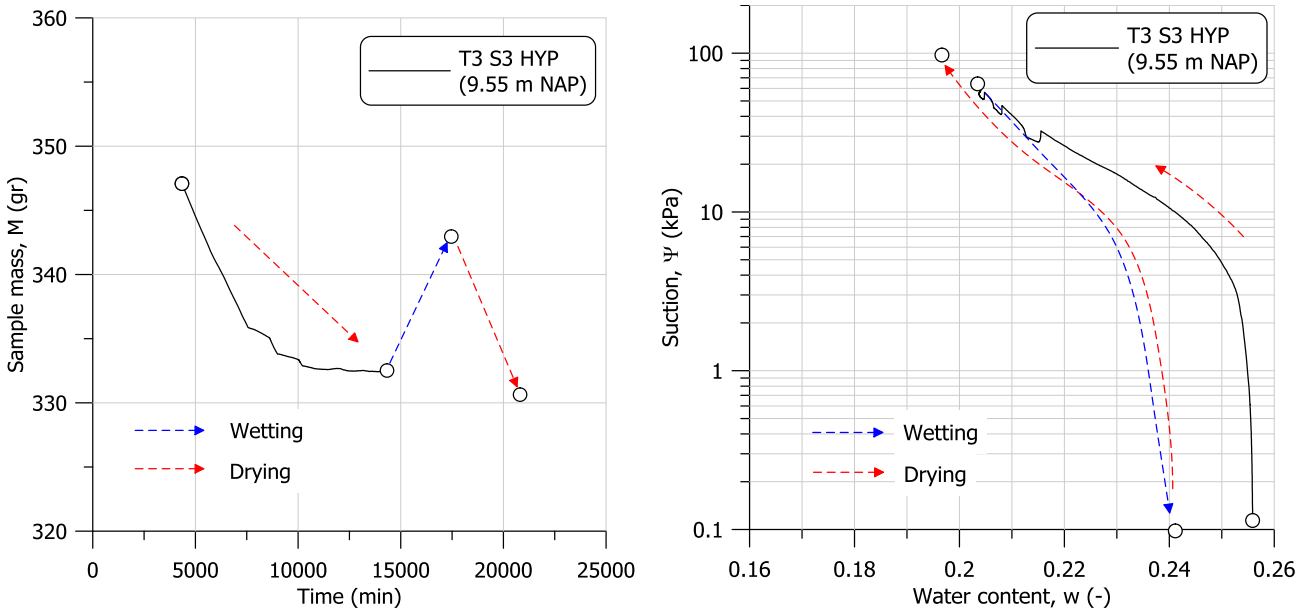

Figure 56. Results of the HYPROP test on sample T3 S3 HYP

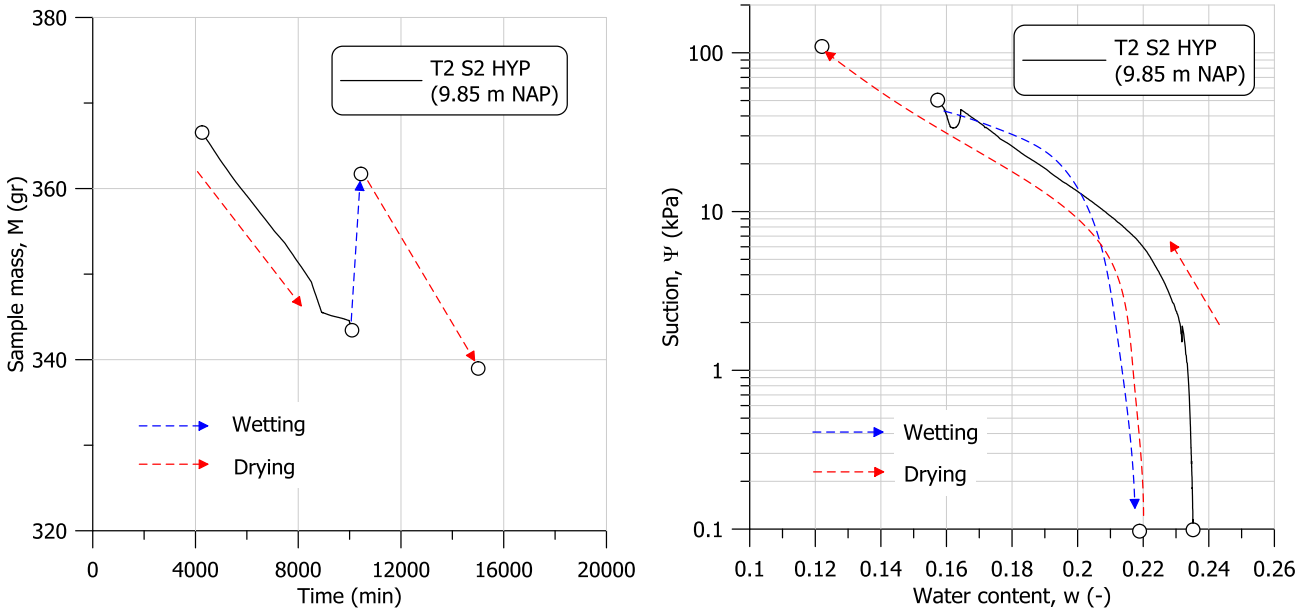

Figure 57. Results of the HYPROP test on sample T2 S2 HYP

5.4. Results of the shrinkage tests

Two shrinkage tests on samples T3 S4 SSC and T5 S3 SSC have been performed to complete the information on the retention properties. The samples, 38 mm in diameter and 38 mm height were dried under controlled conditions, 17°C and 63% relative humidity, for several days. The sample mass and dimensions were measured at regular intervals during drying. Table 19 reports the main index properties of the samples at the beginning of the tests. The shrinkage curves for sample T3 S4

SSC and T5 S3 SSC are displayed in Figure 58 and Figure 59 in terms of void ratio, e, and water ratio, $e_w = wG_s$.

Table 19. Index properties of the samples at the beginning of the shrinkage test

Tube	Sample ID	G_s (-)	w_0 (-)	Averaged depth (m) NAP
3	T3 S4 SSC	2.645	0.294	9.50
5	T5 S3 SSC	2.691	0.347	8.60

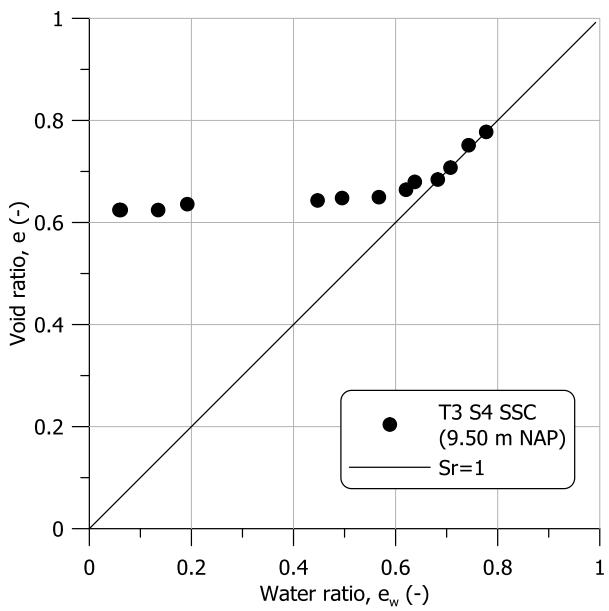

Figure 58. Results of the shrinkage test on sample T3 S4 SSC

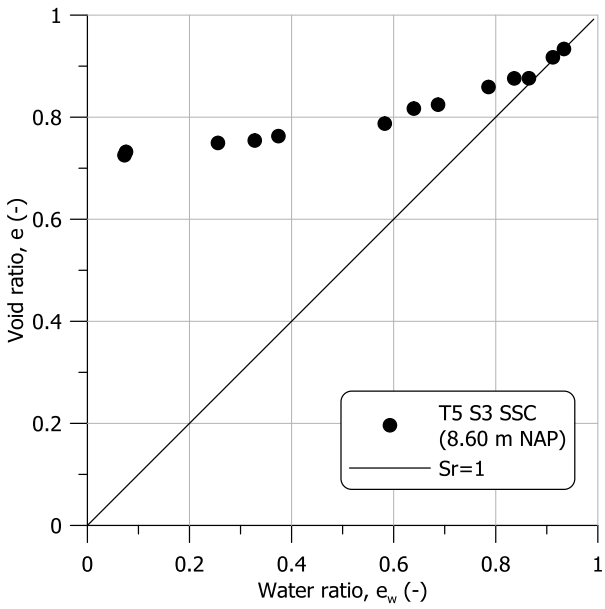

Figure 59. Results of the shrinkage test on sample T5 S3 SSC

6. TUBES PICTURES

6.1. Maasdijk near Oijen

Tube 2

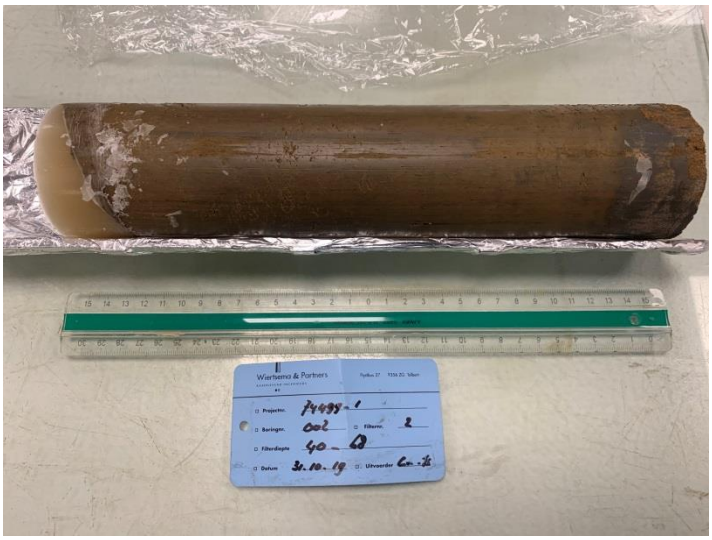

(bottom)

Tube 3

(bottom)

Tube 4

Tube 6

Tube 7

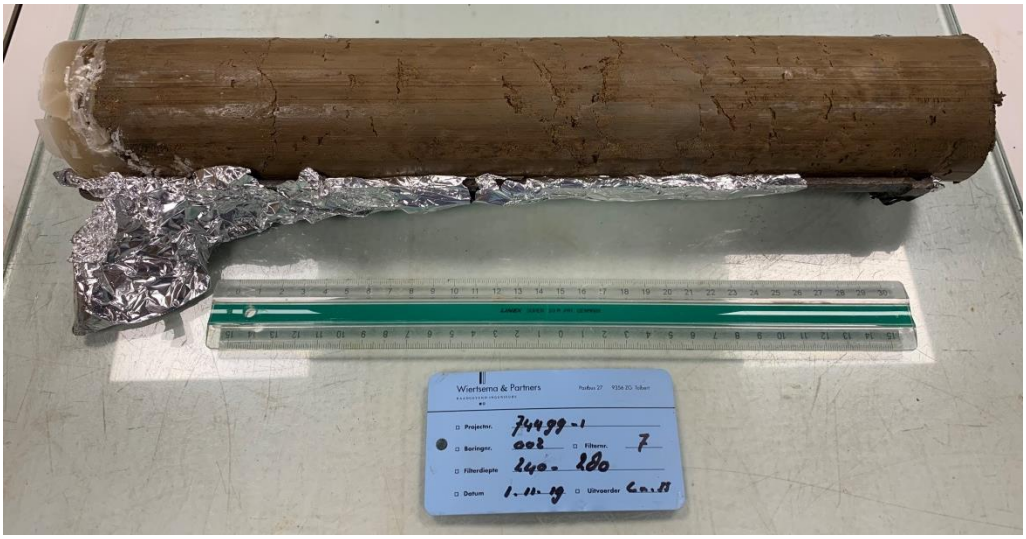

(bottom)

(mid and top)

Tube 9


Wiertsema & Partners
Projectnr.
Boringnr.
002
Filternr.
9
Filterdiepte
320 - 340
Datum
Uitvoerder

6.2. IJsseldijk near Westervoort

Tube 2

Tube 3


Wiertsema & Partners
Projectnr. 7499-1
Boringnr. 202
Filternr. 3
Filterdiepte 0.80 - 1.19
Datum 11-8-20
Uitvoerder JuJo

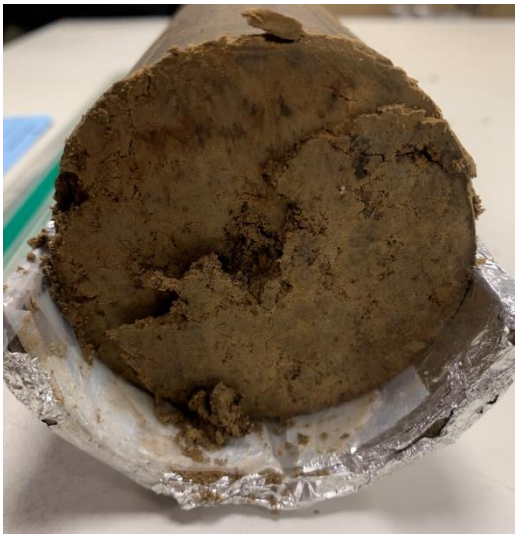

Tube 4

Tube 5

Reference

Fukushima, S. and Tatsuoka, F., (1984). Strength and deformation characteristics of saturated sand at extremely low pressure. Soils and foundations, Vol. 24, No. 4, pp. 30-48.

Grondmechanica Delft. (1996). Onderzoek stabiliteit Maasdijken, Vak D, Oijen Benedeneind – Zuiveringsinstal. HM 574 tot HM 595. Geotechnisch Profiel G-G'. Project CO-361580.

La Rochelle, P., Leroueil, S., Trak, B., Blais-Leroux, L. and Tavenas, F. (1988). Observational approach to membrane and area corrections in triaxial tests. Advanced triaxial testing of soil and rock, Donaghe, Chaney Silver eds.

Inpijn-Blokpoel. (2017). Grondonderzoek voor de 4e toetsronde - Resultaten geotechnisch onderzoek. Documentnummer 02P008040-RG-01. 1 augustus 2017.

Tollenaar, R. N., van Paassen, L. A., and Jommi, C. (2018). Small-scale evaporation tests on clay: influence of drying rate on clayey soil layer. Canadian Geotechnical Journal, 55(3), 437-445.

Muraro S, Jommi C (2019) Experimental determination of shear strength of peat from standard undrained triaxial tests: correcting for the effects of end restraint. Géotechnique. https://www.icevirtuallibrary.com/doi/10.1680/jgeot.18.P.346 (ahead of print).

HYPROP© UMS GMBH MUNICH, (2015). User Manual Hyprop. www.umsmuc.de Versi0n 2015_01.

van Duinen, A. (2020). Shear Strength of Initially Unsaturated Soil - Results measurements Oijen and Westervoort. 11204453-002-GEO-0001, Version 2.0, March 21, 2020, Deltares.